Marine Micropaleontology 201 (2025) 102518

Contents lists available at ScienceDirect

Marine Micropaleontology

journal homepage: www.elsevier.com/locate/marmicro

Insights into the spatial and vertical distribution of extant planktonic foraminifera in the Bay of Bengal

Rose Manceau [a,b,*], Meryem Mojtahid [a], Eelco Rohling [c,d], Robin Fentimen [a], Thibault de Garidel-Thoron [e], Sonia Chaabane [e,f,g], Gianluca Marino [h]

[a] Univ Angers, Univ Nantes, Univ Le Mans, CNRS, LPG, Laboratoire de Planétologie et Géosciences, UMR 6112, 2 Bd Lavoisier, 49045 Angers Cedex, France
[b] Research School of Earth Sciences, The Australian National University, Canberra, ACT, 2601, Australia
[c] Department of Earth Sciences, Utrecht University, Vening Meinesz building A, Princetonlaan 8a, 3584 CB Utrecht, The Netherlands
[d] Ocean and Earth Science, University of Southampton, National Oceanography Centre, Southampton SO14 3ZH, UK
[e] Aix-Marseille Université, CNRS, IRD, Collège de France, INRAE, CEREGE, Aix-en-Provence, France
[f] Department of Climate Geochemistry, Max Planck Institute for Chemistry, Germany
[g] Fondation pour la recherche sur la biodiversité (FRB-CESAB), France
[h] Centro de Investigación Mariña, GEOMA, Palaeoclimatology Lab, Universidade de Vigo, Vigo 3610, Spain

ARTICLE INFO

Keywords:
Planktonic foraminifera
Bay of Bengal
Plankton net
Sediment trap
Ganges-Brahmaputra River
Depth habitat
Vertical distribution
Indian Monsoon

ABSTRACT

Planktonic foraminifera provide essential palaeoceanographic proxies, as their shells are used to characterise past ocean conditions. The accurate interpretation of palaeorecords depends on a thorough understanding of the species-specific ecological preferences. While global distribution patterns are well documented, regional analysis are sparser, which limits our understanding of the response of planktonic foraminiferal distribution to local environmental conditions. This study synthesises data of extant planktonic foraminiferal abundances to determine their spatial and vertical distributions in the Bay of Bengal, using available and published plankton net and sediment trap data. Our analysis highlights the dominance of six species that exhibit distinctive spatial and vertical distribution patterns. *Globigerinoides ruber* and *Trilobatus sacculifer* are associated with oligotrophic waters, and nutrient-rich areas, respectively. They consistently inhabit the upper 40 m of the water column, within the mixed layer. *Neogloboquadrina dutertrei* and *Globigerina bulloides* thrive in stratified waters near the Ganges-Brahmaputra River mouth and in the upwelling system south of India. While abundant in the mixed layer, their high numbers in the subsurface in stratified conditions and associated subsurface nutrient availability highlights their capacity to dwell in both surface and subsurface environments. *Globorotalia cultrata* and *Globigerinita glutinata* are abundant in the northern Bay of Bengal, with *G. cultrata* inhabiting the upper thermocline, while *G. glutinata* has the broadest vertical distribution, from the mixed layer to the deep thermocline. These findings help constraining the regional response of key species to local conditions and hence their use in palaeoenvironmental reconstructions from this critical sector of the global ocean.

1. Introduction

Planktonic foraminifera (PF) are protozoans that inhabit the global ocean, ranging primarily from surface to sub-thermocline depths (e.g., Fairbanks et al., 1980, 1982; Kuroyanagi and Kawahata, 2004; Bergami et al., 2009; Iwasaki et al., 2017; Rebotim et al., 2017). Their calcareous shells are widely used as palaeoceanographic proxies through the analysis of fossil assemblages and species-specific shell geochemistry (e.g., Emiliani, 1955; Nürnberg et al., 1996; Kucera, 2007; Schiebel and Hemleben, 2017). The interpretation of proxies derived from fossil PF (based on assemblages or geochemical signature of their tests) requires understanding of their present-day ecological preferences, hence their spatial and depth distribution (e.g., Duplessy et al., 1981; Seears et al., 2012; Rebotim et al., 2017; Kretschmer et al., 2018; Stainbank et al., 2019). The depth habitat and the calcification depths of PF species vary regionally and are not globally uniform (e.g., Peeters and Brummer, 2002a, 2002b; Rebotim et al., 2017; Stainbank et al., 2019), making regional documentation of habitat variability essential to allow robust

* Corresponding author at: Univ Angers, Univ Nantes, Univ Le Mans, CNRS, LPG, Laboratoire de Planétologie et Géosciences, UMR 6112, 2 Bd Lavoisier, 49045 Angers Cedex, France.
E-mail address: rose.manceau@univ-angers.fr (R. Manceau).

https://doi.org/10.1016/j.marmicro.2025.102518
Received 15 April 2025; Received in revised form 19 September 2025; Accepted 22 September 2025
Available online 25 September 2025

palaeoceanographic reconstructions (e.g., Lynch-Stieglitz et al., 2015; Raddatz et al., 2017).

On the global scale, the modern spatial distributions of PF species composition is closely tied to ocean surface temperature, and the fossil assemblages reveal that these distributions shifted in response to past temperature changes (e.g., Bé and Tolderlund, 1971; Bé and Hutson, 1977; Kipp, 1976; Chaabane et al., 2024; Jonkers et al., 2023, 2024). Data from plankton tows and sediment traps unveil that the composition and abundance of living PF communities are also influenced by other environmental factors, including food availability, light intensity, salinity, and water column stratification (e.g., Ortiz et al., 1995; Schiebel et al., 2001; Field et al., 2006; Jonkers and Kučera, 2015, 2017; Rebotim et al., 2017; Lessa et al., 2020). These influences are most evident in regions affected by upwelling, boundary currents, hydrographic fronts, or sharp turbidity and salinity gradients. In such environments, certain species appear to be tolerant to a wide range of environmental conditions. For example, the *Globigerinoides ruber* subspecies (*albus* and *ruber*) tolerate a wide range of temperature and salinity (Bijma et al., 1990b). They typically inhabit tropical to subtropical surface waters in highly saline oligotrophic areas and can also be found in nutrient rich low-salinity waters, influenced by rivers. As a result, this euryhaline taxon is ecologically competitive and widely present in different low and even mid-latitudes hydrographic settings (e.g., Ufkes et al., 1998; Schmuker and Schiebel, 2002; Morard et al., 2019). The vertical distribution of PF in the water column is overall less well documented than their horizontal distribution. Recent studies have addressed this gap by examining the environmental factors that influence PF vertical distribution (Rebotim et al., 2017; Lessa et al., 2020; Tapia et al., 2022; Chaabane et al., 2025). These studies using vertically resolved plankton tows concluded that light intensity, water temperature, oxygen and food availability, nutrient levels, and predation are key factors influencing the PF vertical distributions (e.g., Rebotim et al., 2017; Lessa et al., 2020; Tapia et al., 2022). These parameters vary with ocean depth, creating distinct environmental niches, whereby each species occupies a range of depth that can sometimes overlap with other species (e.g., Fairbanks and Wiebe, 1980; Schiebel et al., 2001). The depth habitat of individual species can thus vary significantly depending on the regional setting and on the amplitude and nature of the seasonal cycle. For instance, *Neogloboquadrina dutertrei* has been traditionally interpreted as a subsurface species associated with the deep chlorophyll maximum (DCM) in palaeoceanographic records (Fairbanks et al., 1982). However, vertically resolved plankton tows suggest that this species also inhabits shallower habitat depths under certain hydrographic conditions (e.g., Ufkes et al., 1998; Rebotim et al., 2017). This variability means its depth habitat must be assessed regionally to ensure accurate palaeoceanographic interpretation.

Symbiotic relationship with autotrophic algae is a major factor in defining PF dwelling depth, where photosymbiont-bearing species (usually spinose species, e.g., *G. ruber*, *Trilobatus sacculifer)* occupy surface, light-saturated waters, while photosymbiont-barren species (usually non-spinose species, e.g., *Globorotalia truncatulinoides*) can dwell deeper (Takagi et al., 2019). Species-specific reproduction strategies can drive vertical migration during the lifespan (e.g., sexual reproduction; Erez et al., 1991; Meilland et al., 2021), where mature/big individuals most likely migrate deeper to reproduce and are as such found in the deeper horizon of plankton nets (Meilland et al., 2021). Furthermore, species can seek their optimal habitat by adjusting their position within the water column accordingly (i.e., habitat tracking; Jonkers and Kučera, 2017). Vertical migrations and/or species-specific local habitats can leave an imprint on the stable isotope and/or trace element composition of the PF shells (e.g., Jonkers et al., 2012; Jonkers and Kučera, 2017; Pracht et al., 2019a, 2019b). This may help explain differences of geochemical signatures between different species and may better inform palaeoceanographic interpretations.

This study concentrates on the habitats of extant PF in the Bay of Bengal (BoB), a semi-enclosed basin located in the northeastern Indian Ocean (Fig. 1) that is characterised by dynamic oceanographic and atmospheric circulations (Hood et al., 2024). Intense monsoonal activity over the continent and the northern BoB stems from the seasonal reversal of winds and the northeastern advection of moisture-laden air towards the land masses. This monsoon-driven atmospheric circulation fuels massive, seasonal freshwater discharges from the Himalayan (Ganges and Brahmaputra) and the Indian peninsular (Krishna, Godavari, Mahanadi, Pennar) river systems (Fig. 1; e.g., Chauhan et al., 2004). This produces low-salinity surface-water lenses that propagate meridionally across the BoB, leading to a strong upper water column stratification (Fig. 1; Shenoi et al., 2002, Thadathil et al., 2007; Girishkumar et al., 2011) and the formation of a characteristic density barrier layer (e.g., Vinayachandran, 2002). This climatic and oceanographic setting is targeted by numerous PF-based palaeoceanographic studies to explore past variations in monsoon intensity, biological productivity, and ocean circulation (e.g., Rashid et al., 2007; Rashid et al., 2011; Ahmad et al., 2012; Bolton et al., 2013, 2022; Kumar et al., 2018; Ota et al., 2019; Clemens et al., 2021; Verma et al., 2021; Haridas et al., 2022; Govil et al., 2022). Although a few studies examined the modern ecology of the species that are most commonly used in this research (Belyaeva, 1964; Duplessy et al., 1981; Cullen and Prell, 1984; Guptha et al., 1997; Bhadra and Saraswat, 2021), a comprehensive picture of the control that local (and spatially and seasonally variable) hydrographic conditions exert on the ecological preferences of PF in the BoB is lacking. When using PF species as proxy for reconstructing past ocean conditions in the BoB, it is often assumed that PF have the same ecological requirements and calcification depths as those observed in other low-latitude regions where their ecology has been documented and constrained (e.g., Verma et al., 2022).

To validate these assumptions, we statistically evaluate published plankton tow and sediment trap data that provide a comprehensive picture of the spatial and vertical distribution of key PF species in the BoB (Fig. 2; Belyaeva, 1964; Duplessy et al., 1981; Guptha and Mohan, 1996; Guptha et al., 1997; Munir et al., 2022; Chaabane et al., 2023). Our analysis aims to: (*i*) characterise the composition and spatial distribution of extant PF communities in the BoB in response to locally and regionally changing environmental parameters; (*ii*) assess the link between the PF living depth and vertically resolved environmental parameters such as temperature, salinity, and chlorophyll concentrations; and (*iii*) discuss these findings in the light of PF-based proxies commonly used in palaeoceanographic research. Our findings offer valuable first-order insights into the vertical and spatial habitat preferences of key PF species in the BoB, which can guide future efforts to refine geochemical proxy interpretations under varying environmental conditions.

2. Study area

2.1. Surface hydrography

The BoB is a semi-enclosed basin in the northeast Indian Ocean, and its surface hydrography is primarily controlled by the Indian monsoon. This system is characterised by seasonal wind reversals, which drive surface ocean circulation and rainfall precipitation, along with the associated river discharge (Fig. 1; e.g., Pédelaborde, 1963; Schott and McCreary Jr., 2001; Schott et al., 2009). The BoB receives substantial freshwater input from direct monsoonal rainfall (~6400 km^3/year; Chaitanya et al., 2021) and runoff (~3020 km^3/year; Chaitanya et al., 2021) from major river systems, including the Ganges and Brahmaputra in the north, the Krishna, Godavari, Mahanadi, and Pennar rivers along India's eastern coast, and the Irrawaddy and Salween rivers in the Andaman Sea (e.g., Chauhan et al., 2004; Fig. 1). This influx is most pronounced during the summer monsoon (e.g., Gomes et al., 2000; Narvekar and Prasanna Kumar, 2014; Sarma et al., 2016). The BoB is a dilution basin, as freshwater inputs from direct precipitation and continental runoff exceed evaporation (Ding et al., 2004; Paul et al., 2007;

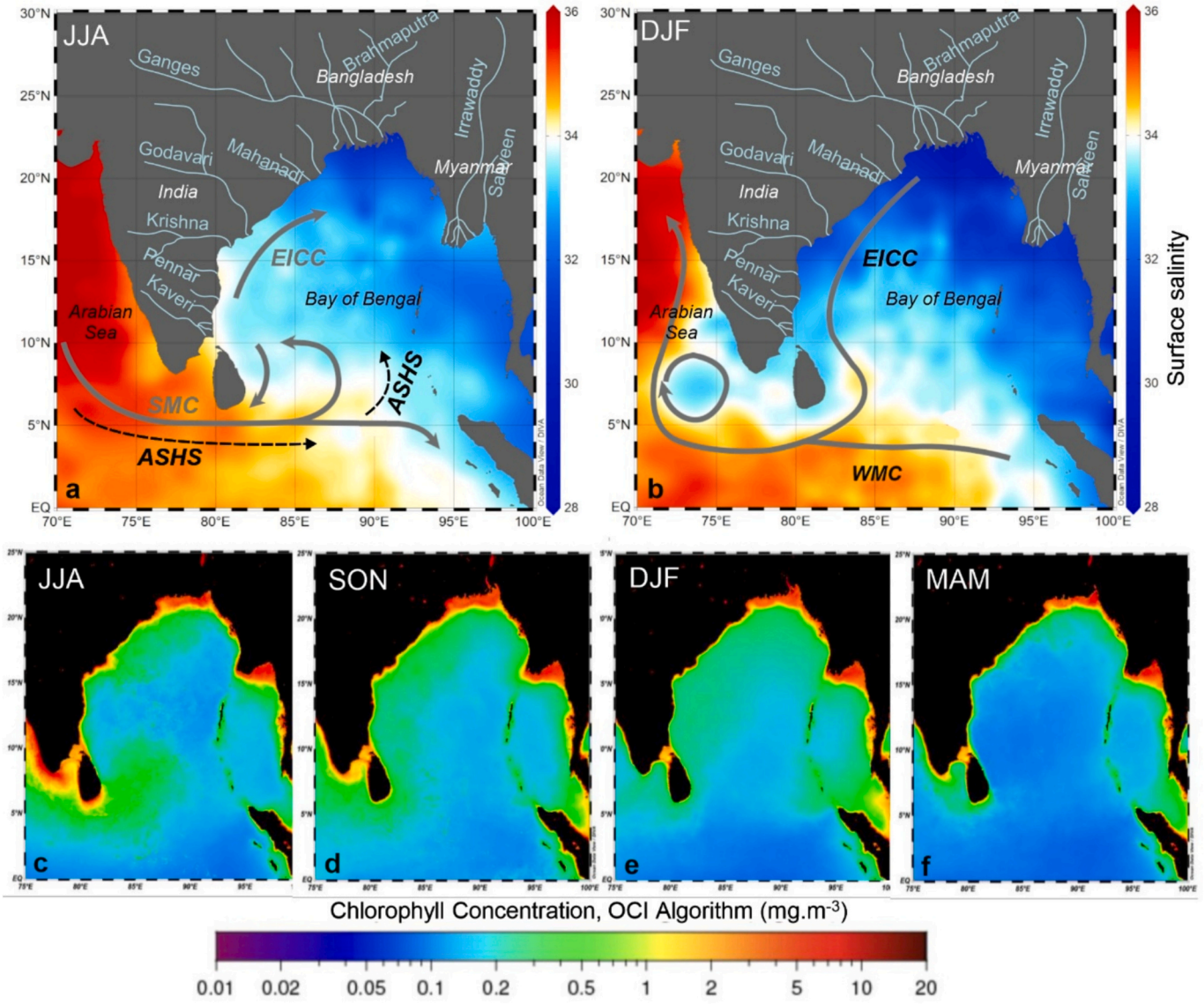

Fig. 1. Seasonal variations in surface salinity and chlorophyll-a concentration in the Bay of Bengal. Seasonal climatology of surface salinity averaged over the 1927–2018 period (World Ocean Database [WOD18], Boyer et al., 2018). a) Boreal summer (June, July, August – JJA) and b) boreal winter (December, January, February – DJF). Contour maps were generated using Ocean Data View (ODV, Schlitzer *et al.*, 2018). Seasonal surface ocean circulation patterns are also illustrated (grey lines and arrows, Schott et al., 2001): East India Coastal Current (EICC); Winter Monsoon Current (WMC); and Summer Monsoon Current (SMC, sometimes referred to as North Equatorial Current [NEC]; Schott and McCreary Jr., 2001; Schott et al., 2001). Seasonal satellite-derived chlorophyll-a concentrations from the MODIS-Aqua Level-3 dataset (https://oceancolor.gsfc.nasa.gov/): c) satellite chlorophyll-a concentration data during summer; d) fall (September, October, November – SON); e) winter; and f) spring (March, April, May – MAM).

Chaitanya et al., 2021). The extensive (and seasonally biased) freshwater discharge creates a strong NE-SW salinity gradient, which ranges from ~20 near river mouths to ~34 in the south (Shetye et al., 1993; Akhil et al., 2014). Surface freshening also induces a strong, near-surface haline stratification that dampens the seasonal variations in mixed layer depth (e.g., Gomes et al., 2000; Prasanna Kumar et al., 2002a, 2002b; Narvekar and Prasanna Kumar, 2014; Sarma et al., 2016), notably in the northern BoB (Dandapat et al., 2021), where a characteristic barrier layer forms between the shallow mixed layer and the top of the thermocline (Vinayachandran, 2002; Kumari et al., 2018). This feature helps maintain surface temperature above 28°C by inhibiting heat exchange between the atmosphere and the deeper layers of the ocean (Shenoi et al., 2002).

Surface circulation varies seasonally, from anticyclonic during the summer monsoon to cyclonic during the winter monsoon (Hood et al., 2024). From May to August (boreal spring and summer), the northward-flowing East India Coastal Current (EICC) (e.g., Schott and McCreary Jr., 2001; Schott et al., 2009; Fig. 1) and the eastward South Monsoon Current (SMC) dominate (Schott and McCreary Jr., 2001; Schott et al., 2009; Fig. 1). In fall (September–November), as the summer monsoon retreats, northeasterly winds establish along with an equatorward EICC and westward Winter Monsoon Current (WMC) (Schott and McCreary Jr., 2001; Fig. 1). This pattern continues through winter (December–February), allowing low-salinity surface water to propagate southward (Vinayachandran et al., 1999; Shankar et al., 2002; Fournier et al., 2017).

2.2. Primary productivity

Productivity in the BoB is influenced by wind patterns, surface and deep ocean circulation, advection of nutrient-rich waters from the Arabian Sea, and river runoff (e.g., Vinayachandran, 2009; Chowdhury

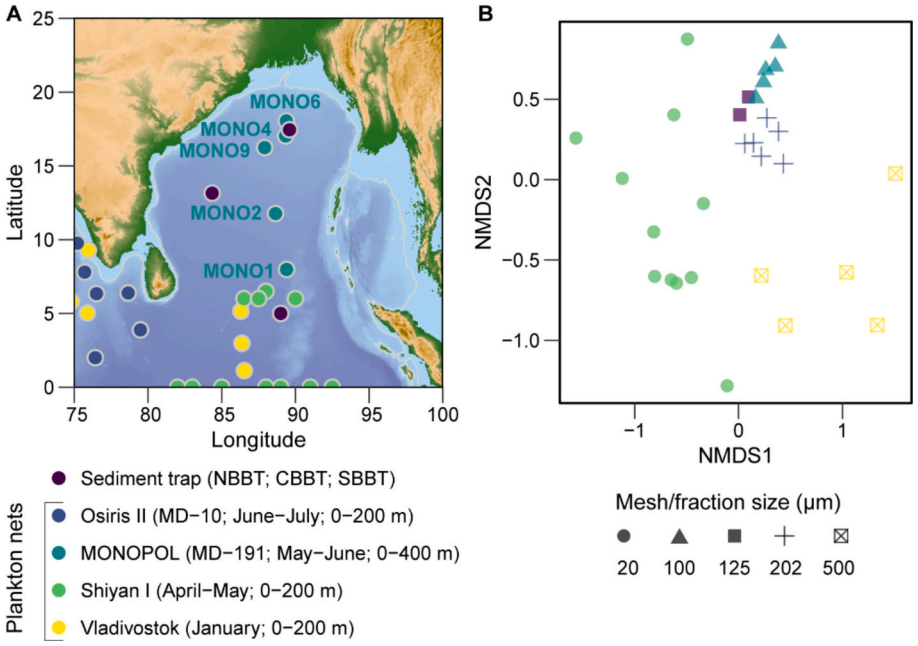

Fig. 2. A- Inventory and locations of the missions and the associated plankton nets and sediment traps deployed in the Bay of Bengal. The MONOPOL stations used to analyse the vertical distributions of planktonic foraminifera are also indicated. B- NMDS ordination based on the dissimilarity distance (Bray-Curtis) between samples. NMDS is performed on samples based on planktonic foraminifera relative abundance to include all missions. For consistency, a subset of 0-180 m for MONOPOL was used to harmonise with the depth ranges of other missions. The NMDS colour code corresponds to the different missions.

et al., 2021). Overall, the BoB is oligotrophic due to strong salinity stratification, especially in the north (during the southwest monsoon), where (sustained) river runoff influences the surface hydrology. The strong stratification limits the vertical transfer of nutrients, restricting their availability for phytoplankton (e.g., Gomes et al., 2000; Prasanna Kumar et al., 2004; Vinayachandran, 2009; Löscher, 2021). Additionally, river-borne suspended particles and frequent cloud cover reduce light penetration, thereby limiting the thickness of the photic layer and restricting phytoplankton growth to a thin surface layer (e.g., Prasanna Kumar et al., 2010; Vinayachandran, 2009; Saraswat et al., 2017).

Specifically, in the subsurface, a distinct Deep Chlorophyll Maximum (DCM) forms when stratification is maximum. In the southern BoB, the stratification is easily disrupted by monsoon winds and horizontal advection of high salinity water from the Arabian sea via the SMC (Prasanth et al., 2023), allowing injection of nutrients in the surface, thereby increasing primary productivity. In the northern BoB (north of 18°N), a high year-round stability of the upper water column (i.e. limited vertical mixing) is reported (Chowdhury et al., 2021). As such, during summer monsoon, the wind strengthening cannot break stratification allowing for the DCM to develop in the subsurface (Chowdhury et al., 2021).

Various nutrient sources contribute to seasonal and regional variations in surface primary productivity in the BoB (e.g., Vinayachandran, 2009; Prasanth et al., 2023). From spring and summer (April–September), alongshore SW monsoon winds trigger coastal upwelling along the eastern coast of India (e.g., Shetye et al., 1991; Chauhan and Vogelsang, 2006; Vinayachandran, 2009; 2021). Moreover, the southwesterly winds strengthen in summer and mix the upper water column, mainly in the southern BoB, where salinity-driven stratification is weaker (Thushara et al., 2019). This mixing transports nutrients into the photic zone, enhancing surface primary productivity (e.g., Lévy et al., 2007). Additionally, the Sri Lanka Dome, a cyclonic gyre east of Sri Lanka, drives Ekman pumping, which entrains nutrients into the photic zone and fertilises the area (Vinayachandran et al., 2004; 2009). Massive river runoff during summer supplies significant nutrient inputs to the northern BoB (e.g., Thushara et al., 2019; Chowdhury et al., 2021). However, these nutrients are rapidly consumed and the sinking of organic matter, aided by heavy lithogenic particles, limits offshore transport (Singh et al., 2012; Singh and Ramesh, 2011; Krishna et al., 2016; Prasanna Kumar et al., 2004; Ittekkot, 1993; Löscher, 2021). In fall (September-November), the southward flowing EICC redistributes river-borne nutrients from the Ganges-Brahmaputra and other coastal river systems along the western margin of the BoB (Vinayachandran, 2009; Fournier et al., 2017). November is also marked by increased tropical cyclone activity, often leading to localised phytoplankton blooms (Vinayachandran and Mathew, 2003; Siswanto et al., 2023). During winter, weaker northeasterly winds, compared to the strong summer southwesterlies, result in a small secondary peak in productivity (e.g., Lévy et al., 2007).

3. Materiel and methods

3.1. *Modern planktonic foraminifera database*

3.1.1. *Data inventory*

For a modern PF census in the BoB (0–25°N, 75–100°N), we extracted plankton tow and sediment trap data from the FORCIS database (Fig. 2; Table 1; de Garidel-Thoron et al., 2022; Chaabane et al., 2023) and literature sources (Munir et al., 2022; Maeda et al., 2022). Plankton tows were deployed during various scientific cruises across different seasons (Table 1):

- Spring (April–May): Shiyan I (Munir et al., 2022)
- Transition between spring and summer (May–June): MONOPOL, MD-191 (Bassinot and Luc, 2012)
- Summer, during the peak of the summer monsoon (June–July): OSIRIS II (Duplessy et al., 1981)
- Winter, under winter monsoon conditions (January): Vladivostok (Belyaeva, 1964)

Among these data sets, MONOPOL MultiNet transect (included in Chaabane et al., 2023) is analysed here for the first time to vertically resolve the PF depth distribution.

Three sediment traps (Table 1) were deployed in the northern

Table 1
Inventory of missions that deployed tows and sediment traps in the BoB. ML* (mixed layer), Multinet** (precision about the deployment of plankton nets during the MONOPOL is given in Section 3.2). >150*** μm corresponds to the fraction analysed in Maeda et al. (2022a), which shares a time interval with Guptha et al. (1997) study.

Mission	Date	Location	Season	Depth (m)	Size fraction (μm)	Sampling method	Reference
Vladivostok	01/1960-02/1960	Southern tip of India and southern BoB 1.1-9.2°N 74.8-86.5°E	Winter	0–200	> 500	Plankton net	Belyaeva (1964)
OSIRIS II (MD10)	06/1976-07/1976	Southern tip of Inia 2-9.7°N 75.2-79.5°E	Summer	0–200	>202	Plankton net Cast in the ML* and below the ML*	Duplessy et al. (1981)
MONOPOL (MD191)	05/2012-06/2012	Central BoB 8-18°N ~90°E	Spring and summer	0–400	>100	Multinet** 2 casts (described in the text)	Bassinot and Beaufort (2012)
SHIYAN I	04/2014-05/2014	Southern to equatorial BoB 0-6.5°N 82-92.5°E	Spring	0–200	>20	Plankton net	Munir et al. (2022)
NBBT	11/1988- 11/1989	Northern BoB 17.5°N-89.6°E		967 2029	>125	Sediment trap	Guptha et al. (1997)
CBBT	11/1988- 11/1989	Central BoB 13.1°N-84.3°E		950 2160	>125 >150*** >125	Sediment trap	Guptha et al. (1997), Maeda et al., 2022***
	12/1990-10/1991			893	>150***		
	01/1993-10/1993			899	>150***		
SBBT	02/1992-12/1992	Southern BoB 5°N-87°E		1518	>125	Sediment trap	Guptha and Mohan (1996)

(NBBT), central (CBBT), and southern (SBBT) BoB (Guptha and Mohan, 1996; Guptha et al., 1997; Maeda et al., 2022). At NBBT, multiple traps collected monthly samples over the course of a year, while at CBBT, several years of monthly samples were obtained. In contrast, SBBT was sampled by a single mooring that covers about a year of monthly sampling (Table 1; Guptha and Mohan, 1996; Guptha et al., 1997; Maeda et al., 2022).

In summary, we analyse data from 30 stations, which cover the equatorial region, the transition between the Arabian Sea and the BoB around the southern tip of India, and a longitudinal transect near 90°E in the central BoB. Of these, five stations (MONOPOL) allow evaluation of the vertical PF distributions in 20-m increments from 0 to 100 m, and until 400 m with lower-resolution increments (100–180 m; 180–400 m). Six stations (OSIRIS II) were deployed once in the mixed layer (0-80 m) and once in the thermocline (80–200 m), and three sediment trap stations document seasonal fluxes (Guptha and Mohan, 1996; Guptha et al., 1997; Maeda et al., 2022).

3.1.2. Taxonomic harmonisation

All species count were generated for 'lumped' taxonomy proposed by the FORCIS group (Chaabane et al., 2023), which follows the recommendations of Brummer and Kučera (2022), Morard et al. (2019), and Schiebel and Hemleben (2017). Recently, the taxonomy has recognised the previously assigned morphospecies *Globigerinoides ruber* sensu lato (Wang, 2000) as the genetic species *Globigerinoides elongatus* (d'Orbigny, 1826, Morard et al., 2019). However, the published datasets (Belyaeva, 1964; Duplessy et al., 1981) in our study region do not differentiate *G. elongatus* from *G. ruber albus* (Morard et al., 2019; the latter previously referred to as *G. ruber sensu stricto*, respectively). For this study, some species were lumped together for data analysis, such as *G. ruber* (*Globigerinoides ruber albus* + *Globigerinoides elongatus*), and *T. sacculifer* (*T. sacculifer* no sac + *T. sacculifer* with sac). Some synonyms that differ from the proposed taxonomy of Brummer and Kučera (2022) were found in the FORCIS database. We kept the name *Globorotaloides hexagona* instead of *Globorotaloides hexagonus,* and the synonym *Globorotalia theyeri* instead of *Globorotalia eastropacia, Globorotalia cultrata* instead of *Globorotalia menardii* (Brummer and Kučera, 2022). We harmonised the taxonomy of the Shiyan database (Munir et al., 2022) with the FORCIS taxonomy using the synonyms list of Brummer and Kučera (2022). We provide a list of the extant species observed in our study area as Supplementary Material S1.

3.1.3. Data extraction, and selection criteria

Using the FORCIS package (Casajus et al., 2025), in R (version 4.4.0; 2024-04-24) we extracted the absolute abundances of PF species at each station using the function compute_concentrations() (Fig. 3; Fig. 4). No distinction was made between living and dead organisms, and taxonomic completeness was assured according to the FORCIS database, apart from the sediment trap where counts of unidentified individuals were reported.

Because the MONOPOL stations (Bassinot and Luc, 2012) were deployed down to 400 m depth, we used a subset of the data from 0 to 180 m depth to harmonise them with the plankton nets from other missions when describing spatial distribution (Fig. 3). We calculated relative abundance to characterise spatial distribution to ensure comparability with fossil assemblages and remove differences that arise solely from variation in total abundances between stations, which are not explicable by in situ CTD data (e.g., Yu et al., 2017). For the sediment trap time-series, relative abundances presented in Fig. 3 were calculated from a subset of data corresponding to the months of May and June, using specimens in the >125 μm size fraction, and including the unidentified specimens. This was done to ensure consistency with other "plankton datasets" that are used in the vertical distribution analysis, particularly MONOPOL. To assess seasonal and interannual variability of the main PF species detected in this study (see below), we show sediment fluxes and relative abundance time-series over several years, extracted from FORCIS database and from Maeda et al., 2022 (Fig. 3B and C).

3.1.4. Dataset validation

Due to disparities in sampling effort, such as differences in sampling season, plankton net mesh size, and taxonomy (discussed above), we

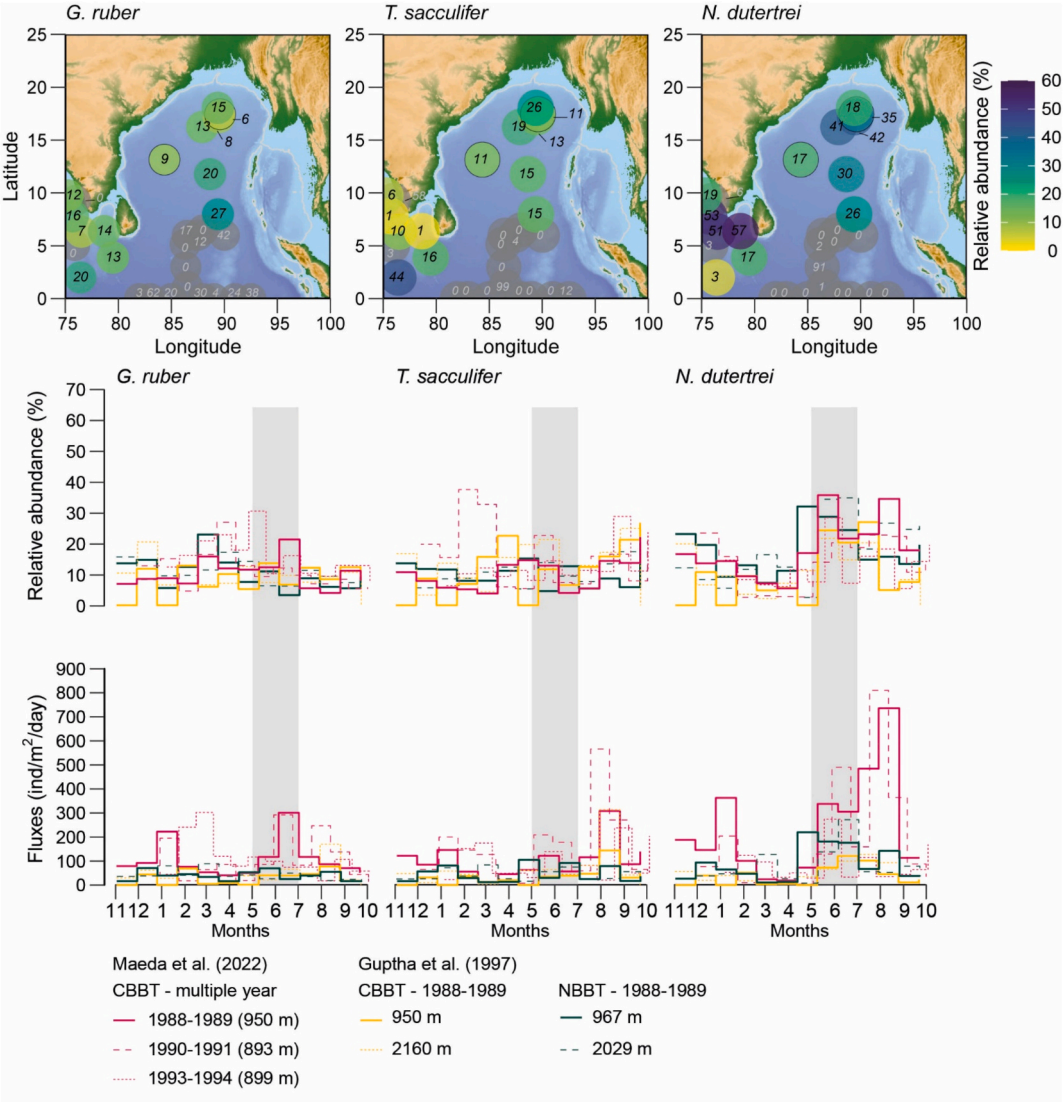

Fig. 3. Relative abundance (%) and associated fluxes of the six dominant planktonic foraminifera species in the Bay of Bengal, in plankton nets and sediment traps. The map shows average relative abundances for CBBT and NBBT over May-June (circled in black); grey points correspond to data from missions that did not pass the quality check (cf. Section 3.1.4). Flux data are from Guptha et al. (1997) and Maeda et al., 2022a. Months of May and June are highlighted by the grey panels. Note that relative abundance data for SBBT are not shown as flux data were available only for *G. bulloides* (Gupta and Mohan, 1996). The base map was produced using the marmap package and ggplot2 (v1.0.10; Pante and Simon-Bouhet, 2013; Wickham et al., 2025).

statistically tested whether these factors influence the observed assemblage structure, and in turn, our interpretation. First, we calculated the Bray-Curtis dissimilarity index between assemblages' relative abundances using the vegan package (Oksanen et al., 2024) in R (v4.4.0). This allowed inclusion of all missions regardless of absolute abundance data availability (Fig. 2). Second, we performed a PERMANOVA (Permutational analysis of variance) to test the influence of the mesh size on the assemblage's variance.

3.2. Depth habitat of planktonic foraminifera

With the vertically resolved MONOPOL plankton nets, two deployments were made successively at each of the 5 stations. The first deployment consists of a high-resolution sampling every 20 m in the uppermost 100 m of the water column. The second deployment consists of lower resolution, deeper sampling, usually at 60-80 m, 80-100 m, 100-180 m, and 180-400 m. Two stations (MONO2 and MONO4) were also sampled in the 0-60 m depth interval during the second cast. For the characterisation of PF depth habitats, here we combine data from the first and second deployments. We calculate the average absolute and relative abundance of the two casts within the same depth interval (common depth interval between 60-80 and 80-100 m). In order to describe the PF depth habitat (DH), we use the species absolute abundance (individuals per cubic metre - ind/m^3) at different depth intervals from all deployments (Fig. 4).

Following the approach of Rebotim et al. (2017) and Greco et al. (2019), the DH and vertical dispersion range (VDR) were calculated for PF species with more than five individuals per station (Figs. 4 and 5). In this study, DH was calculated without distinguishing between living and dead specimens, due to the lack of such differentiation in the available data. The DH is a slight modification from the conventional definition of ALD, which typically refers only to living -cytoplasm-filled- individuals. The DH corresponds to the abundance-weighted average depth where the species occur and was computed using:

$$DH = \frac{\sum Ci.Di}{N}$$

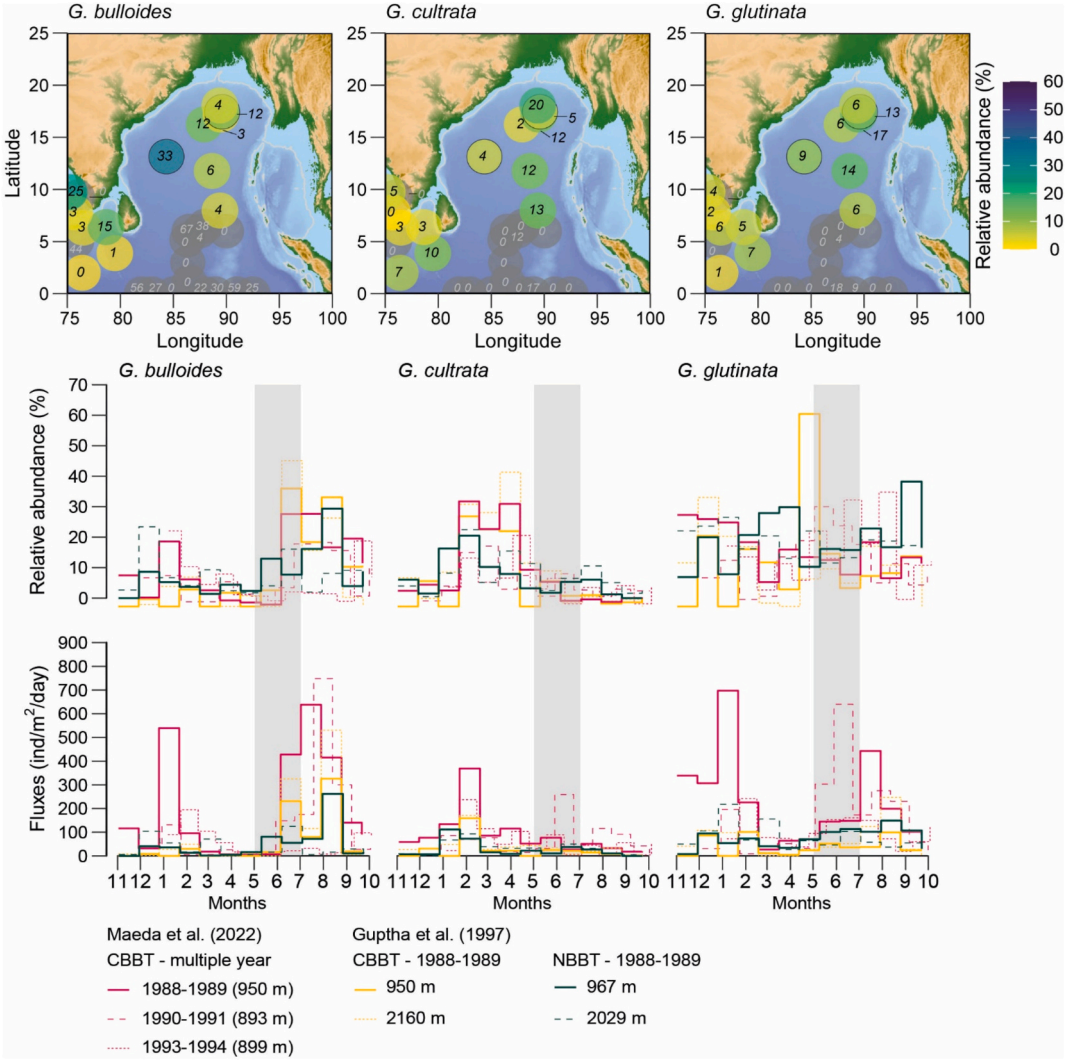

Fig. 3. (*continued*).

where *Ci* is the absolute abundance of individuals per cubic metre at mid-point depth (metre) *Di,* and *N* the total absolute abundance of the species at this station.

At each station, and for each species, we also calculate the DH standard error, where n is the number of observations, i.e. the number of depth intervals:

$$SE = \sqrt{\frac{\sum \left(\frac{Ci}{N}\right).(Di - ALD)^2}{n}}$$

To characterise the vertical distribution of each species in the water column, the VDR was computed, which quantifies the mean deviation of a species' population from its DH (Rebotim et al., 2017; Fig. 4; Table 2), using the formula:

$$VDR = \frac{\sum (|ALD - Di|.Ci)}{N}$$

We calculated weighted skewness (Sk) and excess kurtosis (Kurt) to describe the shape of species' vertical distributions relative to their DH. For each sampling interval *i*, the mid-point depth (*Di*) was taken as the representative depth, and the species concentration (*Ci*) as the statistical weight. Weighted skewness (Sk) and weighted excess kurtosis (Kurt) were then computed as:

$$Sk = \frac{\sum_i Ci(Di - DH)^3}{\sum_i CiSE^3}$$

$$Kurt = \frac{\sum_i Ci(Di - DH)^4}{\sum_i CiSE^4} - 3$$

Skewness and kurtosis together describe the asymmetry and sharpness of the PF depth distribution. Skewness values near zero indicate a symmetric distribution around the DH. Positive skewness means that most individuals are found shallower than the DH, with fewer extending deeper, whereas negative skewness indicates the opposite. Kurtosis measures how strongly individuals are clustered around the DH: higher positive values indicate sharply peaked distributions with occasional occurrences far from the DH, while strongly negative values reflect flatter, more uniform distributions across depths. Ecologically, a strongly positive skewness would suggest a population concentrated near the surface relative to its DH with sporadic deeper individuals, while a strongly negative kurtosis would indicate broad depth tolerance and occupancy of a wide habitat range (Zar, 2014).

We did not discriminate between living and dead specimens, although the presence of dead individuals can bias these metrics towards deeper depths.

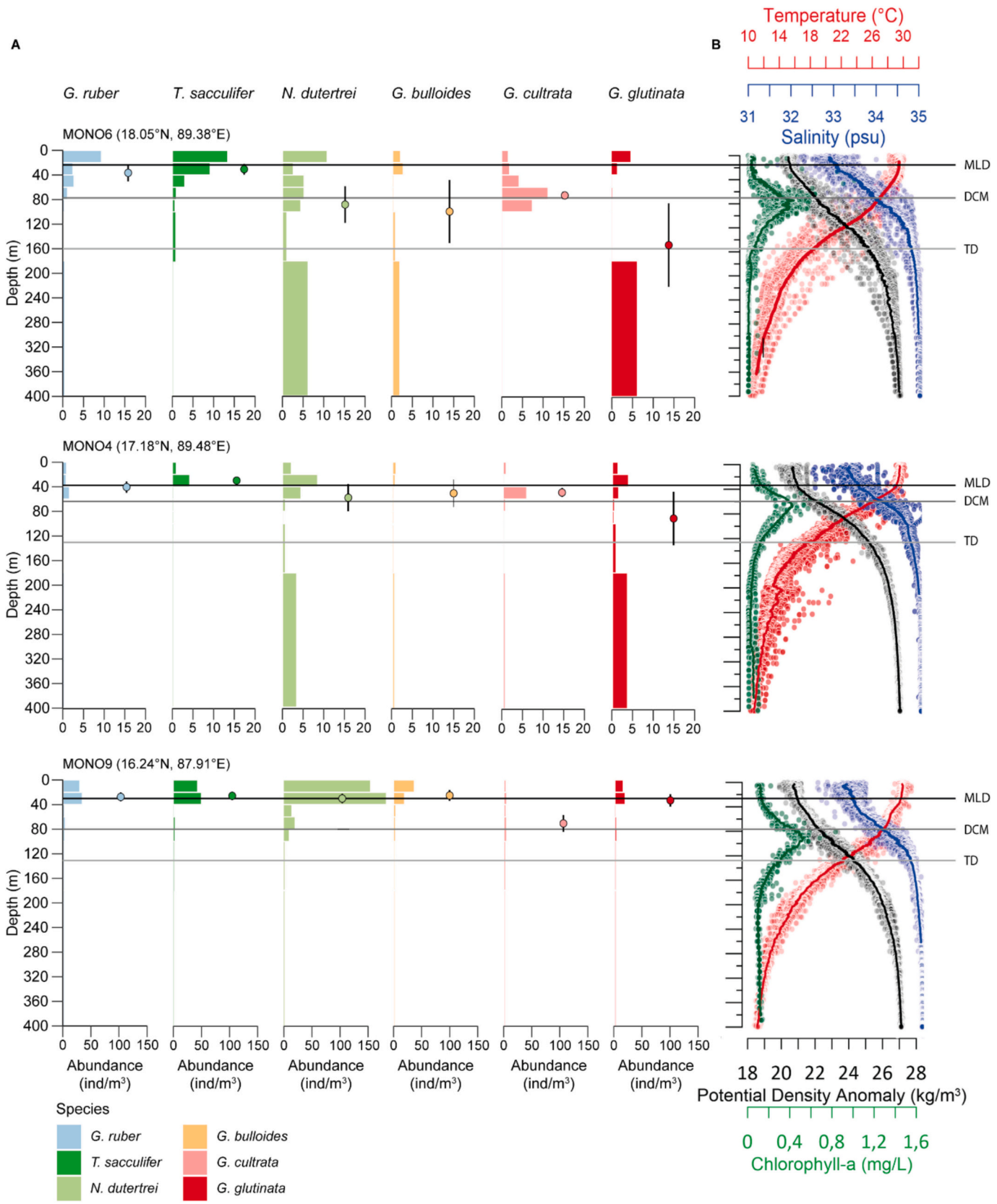

Fig. 4. Vertical distribution of planktonic foraminifera in the Bay of Bengal. A- Absolute abundance of planktonic foraminifera (ind/m^3) at different depths and associated Depth Habitat (DH, circle), and Vertical Dispersion Range (VDR, represented by the vertical bar) of the six dominant PF species. Note the different x-axis scale at station MONO9. B- Hydrographic profiles from April to June of temperature, salinity, density and chlorophyll-a concentration over a 1°x1° grid area around each plankton net deployment site, except for Chlorophyll-a data at MONO1 where a 2°x2° grid area was used. The data were retrieved from WOD (Boyer et al., 2018). The thick coloured lines over the physical parameters represent a moving average. The horizontal dotted lines represent the Mixed Layer Depth (MLD), Deep Chlorophyll Maximum (DCM) depth, and the Thermocline Depth (TD) (cf. material and methods for more details).

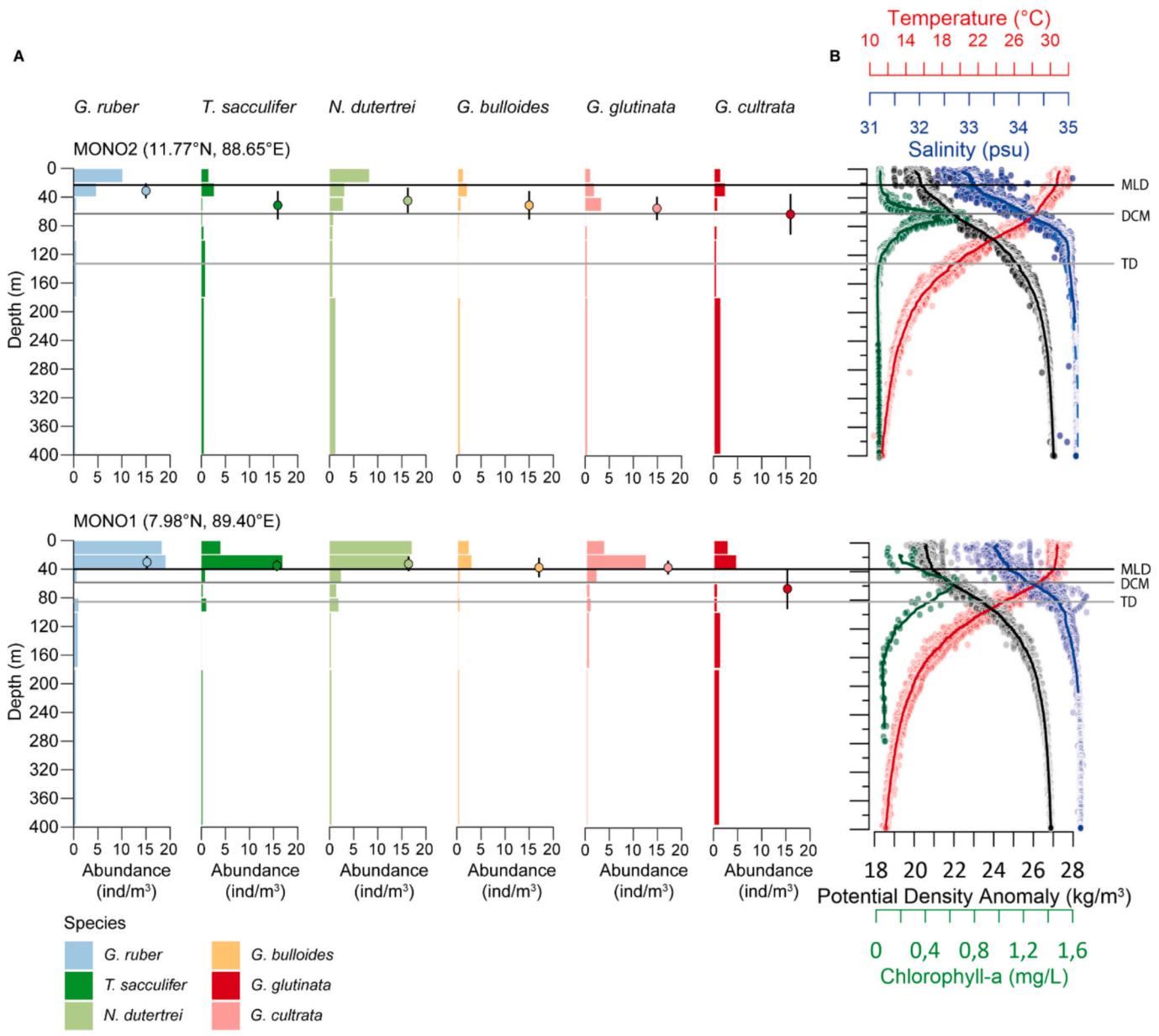

Fig. 4. (*continued*).

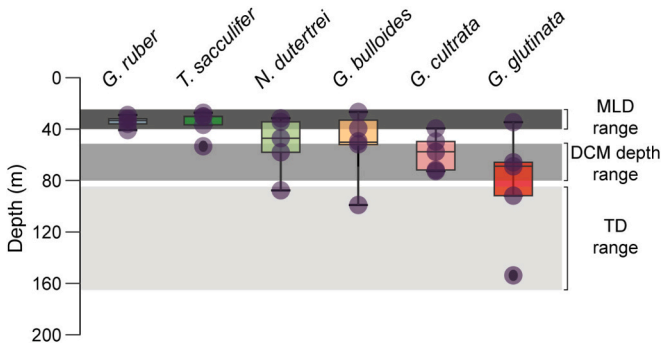

Fig. 5. Overview of dominant planktonic foraminifera depth habitat in the Bay of Bengal (spring 2012). Boxplots of Depth Habitat (DH) are created by combining DH data from all stations. Violet circles indicate the DH at each station. The horizontal grey bands represent the range across the five stations of the Mixed Layer Depth (MLD), the Deep Chlorophyll Maximum (DCM) depth, and the Thermocline Depth (TD).

3.3. Environmental parameters

We used all available data for temperature, salinity, density and chlorophyll-a from the World Ocean Database (WOD18; Boyer et al., 2018) for April to June. The potential density anomaly was calculated using salinity and temperature with the Ocean Data View (ODV) software (Schlitzer, 2023). Water density defines the degree of stratification of the water column, which is a key parameter in the BoB as it influences food availability and trophic structure in the surface and the subsurface (e.g., Vinayachandran et al., 2005; Prasanth et al., 2023). We selected chlorophyll because it represents the distribution of photosynthetic autotrophs, which serve as a food source for some PF (Lipps and Valentine, 1970).

Data was retrieved within a 1°×1° area around each MONOPOL station, except for MONO1, where a 2°×2° area was used to obtain chlorophyll-a data due to its scarcity in that region. These months were selected to include the MONOPOL sampling (May–June) period and the preceding month (April), accounting for the approximate lifespan of planktonic foraminifera (a few weeks to a few months, e.g., Caron et al.,

Table 2
Depth Habitat (DH) and associated standard error (SE), vertical distribution range (VDR), and skewness, excess kurtosis metrics, and mid-depth of the maximum abundance interval (Max. ab. In the table) of the six dominant species at each MONOPOL cruise station, and their average depth habitat over the Bay of Bengal.

Station	Taxa	*G. ruber*	*T. sacculifer*	*N. dutertrei*	*G. bulloides*	*G. cultrata*	*G. glutinata*
MONO1	DH	30	35	33	38	38	68
	SE	13	10	11	17	10	26
	VDR	18	15	20	27	19	57
	Skewness	4.5	5.2	3.8	3.9	3.7	1.9
	Kurtosis	25.1	37.7	23.7	16.1	22.5	2.7
	Max. ab.	30	30	10	30	30	30
MONO2	DH	32	52	46	51	56	64
	SE	13	19	20	22	18	26
	VDR	21	40	36	40	33	57
	Skewness	4.3	2.8	3.1	2.9	3.1	2.2
	Kurtosis	21.5	7.7	9.2	7.1	9.6	3.1
	Max. ab.	10	30	10	30	50	30
MONO4	DH	39	29	57	49	48	91
	SE	14	2	24	24	12	33
	VDR	19	2	44	44	15	87
	Skewness	5.2	-3.5	2.7	2.8	5.5	1.3
	Kurtosis	26.9	10.1	5.6	5.9	32.6	-0.2
	Max. ab.	50	30	30	10	50	30
MONO6	DH	34	29	86	98	71	153
	SE	15	9	29	39	6	0.0
	VDR	28	18	60	103	12	-2.0
	Skewness	4	2.2	1.6	0.9	-1.4	46
	Kurtosis	19.2	5.8	1.2	-1	2.3	137
	Max. ab.	10	10	10	20	70	290
MONO9	DH	27	26	30	25	70	33
	SE	8	7	7	9	14	11
	VDR	14	13	15	18	27	20
	Skewness	4.5	4.8	3.1	4.8	2.3	3.9
	Kurtosis	36.8	42.9	21.9	36.1	10.2	23.8
	Max. ab.	30	30	30	10	70	30
Bay of Bengal	Average DH	33	34	50	32	57	82
	SD	4	11	23	39	14	45

1982; Sykes et al., 2024).

A mean profile is calculated from all available depth data by applying a moving average smoothing method to the data that were rounded and averaged to the nearest tenth meter in order to obtain the same vertical resolution. For the physical parameters (temperature, salinity, and density), a 50-point moving average is used, while for chlorophyll-a concentration, a 20-point moving average is applied. This helps reduce short-term and spatial variability and highlight general trends in the vertical profiles (Fig. 4).

3.4. Linear correlation analysis

To assess the influence of the measured environmental parameters on vertical and spatial distribution of the species at MONOPOL stations, we calculated linear multiple correlations (Pearson correlation) (Fig. 6) using PAST (PAleontological Statistics, 3.08, Hammer et al., 2001). Input for the correlation matrix consists of the DH, of the six dominant species (*Neogloboquardina dutertrei*, *Globigerinoides ruber*, *Trilobatus sacculifer*, *Globorotalia cultrata, Globigerinita glutinata,* and *Globigerina bulloides*) (see section 4.1), and environmental data. Because mixed layer salinity and temperature are similar between stations (Fig. 4), only mixed layer depth (MLD), mixed layer chlorophyll concentration (MLC), thermocline depth (TD), and deep chlorophyll maximum (DCM) depth are considered as environmental variables for multivariate analysis (Table 3). Due to the large number of temperature and salinity profiles, it was not possible to adopt the methodology in which the mixed layer

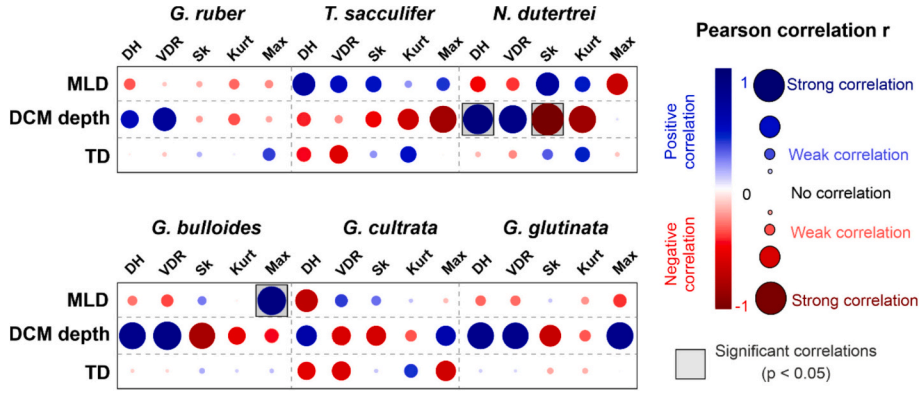

Fig. 6. Linear multiple correlations between planktonic foraminifera data and environmental parameters. Colours refer to Pearson correlation coefficients (*r*), whereby blue indicate positive and red indicate negative correlations. The size and the colour intensity of the symbols are proportional to the strength of the correlation. Significant correlations ($p < 0.05$) are highlighted in grey boxes. Data are provided in Tables 2 and 4. DH: Depth Habitat; VDR: Vertical Depth Range; Sk: Skewness; Kurt: Kurtosis; Max: depth interval mid-point where concentration is maximum; MLD: mixed layer depth; TD: thermocline depth; DCM: deep chlorophyll maximum depth.

Table 3
Ecology of extant planktonic foraminifera in the Bay of Bengal from the literature and the specificities of the Bay of Bengal based on this study.

	General ecology	In the Bay of Bengal
Globigerinoides ruber	Dominant species of the tropical to subtropical water (Bé and Tolderlund, 1971; Bé and Hutson, 1977), that dwells in the mixed layer (Fairbanks et al., 1982; Ravelo et al., 1990). Euryhaline and supporting a wide temperature range under controlled laboratory culture (Hemleben, 1989; Bijma et al., 1990b). Dominant in the freshwater lens of the Amazon/Orinico (Schmuker and Schiebel, 2002). Symbiont-bearing (dinoflagellate) (Hemleben et al., 1989; Takagi et al., 2019). Easily feeds on phytoplankton (Anderson, 1983; Schiebel and Hemleben, 2017)	Preference for the oligotrophic, clear, and more saline waters of the central and southern BoB. Living depth above 40 m.
Trilobatus sacculifer	Dominant species of the tropical to subtropical water (Bé and Tolderlund, 1971; Bé and Hutson, 1977), present in temperate water during summer months (ref; Schiebel et al. 2017). Symbiont-bearing (dinoflagellate) spinose species that dwells in the mixed layer, and that can add gametogenic calcite while descending in the water column (Spezziaferi et al., 2015; Stainbanks et al., 2019). Euryhaline and supporting a wide temperature range under controlled laboratory culture (24-47 psu; 14-32 °C; Hemleben et al., 1989; Bijma et al., 1990b). Present in oligotrophic water. Feeds on calanoid copepod (Hemleben et al., 1989; Schiebel et al., 2017).	Preference for the more productive water near the Indian coastal rivers (Bhadra and Saraswat, 2021), the Ganges-Brahmaputra River (this study), and the southern tip of India. Living mostly in the upper 40 m of the water column.
Neogloboquadrina dutertrei	Common in tropical to subtropical waters and present in temperate waters during summer months (ref; Schiebel et al., 2017). Tolerates a wide range of salinity (25-46 psu) and temperature (13-33°C) in culture experiment, Bijma et al., 1990b). Grows a calcite crust under 15°C that can take up to 70 % of the test wall (Hemleben et al., 1989). Feeds on algae like chrisophytes. Non-spinose symbiont bearing species (*pelagophycae* that requires only low light; Takagi et al., 2029). Surface to upper thermocline dweller, associated to DCM (Faribancks et al., 1982); upwelling system (ref; Schiebel et al., 2004); nutrient-rich river plume in coastal areas (Ufkes et al., 1998).	*N. dutertrei* thrives in the productive water of the upwelling system of the southern tip of India, as well as the vicinity of the nutrient-rich/low-salinity water in the northern BoB. Variable depth habitat, shallow (>50 m) in the central and southern Bay of Bengal, and deeper in northern BoB (up to 86 m).
Globigerinoides bulloides	Associated with transitional to polar water masses and lower latitude upwelling environment (Bé and Hutson, 1977). Usually dwells in the thermocline and above, adding gametogenic calcite while descending in the water columns. Feeds on phytoplankton (Hemleben et al., 1989). Symbiont-barren spinose species with an opportunistic behaviour	Preference for upwelling systems of the southern tip of India (this study; Duplessy et al., 1981). Deeper dwelling depth in the northernmost BoB (~100 m) where low salinity inhibits its presence in surface water.
Globorotalia cultrata	Tropical species that inhabits the deeper mixed layer. Add a variable amount of gametogenic calcite during ontogeny (ref.; Hemleben, 1989;). Feeds on diatoms tintinid and chysophyte (Hemleben, 1989) and chrysophyte.	Associated with the current system of the northern BoB (EICC). Consistently inhabiting the deeper mixed layer to upper thermocline (50-70 m) is associated with DCM.
Globigerinita glutinata	Cosmopolitan species (Bé and Tolderlund., 1971). Calcify from surface to thermocline water while adding gametogenic calcite (Hemleben et al., 1989). Feeds on diatoms and chrysophytes (Schiebel et Hemleben, 2005).	Ubiquitous to the BoB spatially and temporally (this study; Guptha et al., 1997). Variable dwelling depth in the BoB (65 to 90 m).

depth (MLD) is defined as the depth where density changes by a fixed value from the surface. Instead, here, the MLD is established by visual determination of the slope-break, i.e., by identifying the depth where the mean potential density anomaly profile transitions from a well-mixed layer to the stratified pycnocline (e.g., Vinayachandran, 2002; de Boyer Montégut et al., 2004). The MLC represents average chlorophyll concentration in the mixed layer. The TD is identified as the depth where the vertical temperature gradient (dT/dz) is at its maximum (e.g., Yang and Wang, 2009). DCM depth is the depth where the chlorophyll-a concentration is at its highest.

4. Results

4.1. Modern assemblage of planktonic foraminifera in the Bay of Bengal

The two-dimensional NMDS plot (Fig. 2B) shows that assemblages from the MONOPOL and OSIRIS plankton nets, as well as the CBBT and NBBT sediment traps, cluster together despite representing distinct hydrographic regions (summer monsoon upwelling vs. open ocean). In addition, mesh size (or size fraction for sediment traps) explains approximately 15% of the variance. To ensure comparability, we have excluded the VLADIVOSTOK dataset, collected with a 500 μm mesh net, that fails to capture smaller and medium-sized species (e.g., *Globigerinoides ruber*), which are dominant in typical tropical assemblages. Likewise, the Shiyan I dataset, sampled with a 20 μm net, includes small species like *Turborotalia quinqueloba* that are absent from other missions. Moreover, the dominant tropical species *Neogloboquadrina dutertrei* is missing from Shiyan I, likely due to taxonomic misidentification. Given the limitations, we retained only the datasets from OSIRIS, MONOPOL, and the sediment trap studies for further analyses.

The PF assemblages consist of a total of 17 species, showing distinct patterns of abundance across different stations:

- Six are dominant and account for ~60 to ~95% of the total assemblage at most stations: *Neogloboquardina dutertrei, Globigerinoides ruber, Trilobatus sacculifer, Globigerina cultrata, Globigerina glutinata,* and *Globigerina bulloides*.
- Two are common and frequently exceed 5%: *Globigerina siphonifera*, *Globigerina conglobatus*.
- Three are rare and are observed at most stations: *Pulleniatina obliquiloculata*, have relative abundances lower than 5%, and *Globigerinella calida,* and *Hastigerina pelagica* are present with >5% but only at a few stations.
- Six are extremely rare and are observed at fewer than five stations with relative abundance <5%: *Globigerina hexagona*, *Orbulina universa, Globoquadrina conglomerata*, *Globoturborotalita rubescens, Globigerinoides tenellus*, and *Globorotalia theyeri.*

4.2. Spatial distribution of the major planktonic foraminifera species in the Bay of Bengal

The relative abundance of the six dominant PF species is characterised by spatial variations (Fig. 3). *G. ruber* maximum relative abundances are located in the southern sector of the BoB (25.7% at station MONO1). Minimum abundance is found at stations around the southern tip of India (11.62% at station MD10-25), and near the Ganges-Brahmaputra River system (6.4% at NBBT; 8.2% at station MONO4). Conversely, *T. sacculifer* seems more abundant between stations at the south of the tip of India (16% at MD10-17) and near the Ganges-Brahmaputra River mouth (20.6% at station MONO6). *Neogloboquadrina dutertrei* is dominant (56.4% at station MD10-19) around the tip of India and in front of the Ganges-Brahmaputra River system (42.2% at station MONO9). *Globigerina bulloides* is also abundant near the southern tip of India, and along the Equator (25% at MD10-25). *Globorotalia cultrata* and *G. glutinata* seem to follow a similar pattern, with lower relative abundance near the southern tip of India (<10%) and increasing towards the northern BoB, with maximum abundance at the northernmost stations *for G. cultrata* (25.7% at station MONO6) for *G. glutinata* (16.5% at station MONO4). The ecological preferences of these 6 species are presented in Table 4.

4.3. Planktic foraminifera fluxes in the BoB

The sediment trap fluxes of the 6 most abundant species found in the plankton nets are represented along with the averaged relative abundance for the months of May and June that corresponds to the plankton nets sampling period of MONOPOL (Fig. 3; Guptha et al., 1997; Maeda et al., 2022).

Fluxes of *G. ruber* and *T. sacculifer* remain generally low at NBBT with slightly higher fluxes for *T. sacculifer*. At CBBT, their fluxes show a peak centred on August (~175 ind/m^2/day and ~315 ind/m^2/day, respectively). *Neogloboquadrina dutertrei*, and *G. bulloides* show a seasonal signal with more prominent peaks during both monsoon seasons. Regarding the summer peak, it occurs prior to other species with a main peak centred on June at NBBT. *G. glutinata* shows greater fluxes (225 ind/m^2/day) during the winter monsoon at NBBT. This is similar to *G. cultrata* at NBBT and CBBT. These patterns are also observed in the relative abundance of these species.

4.4. Vertical distribution of planktonic foraminifera in the Bay of Bengal

Among the published plankton tows analysed here from the BoB, five plankton nets are resolved vertically. They were deployed on a north-south transect near 90°E in the BoB during mission MONOPOL (Fig. 2; Fig. 4). To estimate the vertical distribution of PF in the BoB we analysed the total concentration of PF at each station (section 4.3.1), the vertical distribution of absolute abundance at the different depth intervals from 0 to 400 m (Section 4.3.2), and the calculated average living depth of the dominant PF species (Section 4.3.3).

4.4.1. Concentrations of dominant species

The highest PF average concentration of ~113 individuals per cubic metre (ind/m^3) are found at station MONO9 (16.24°N, 87.91°E), which is located in the northern part of the BoB. At this station, the PF absolute abundance is approximately 4 to 10 times higher than at other stations. Specifically, average concentrations are ~13 ind/m^3 at stations MONO2 (11.77°N, 88.65°E - central BoB) and MONO4 (17.18°N, 89.48°E-northern BoB), ~25 ind/m^3 at station MONO1 (7.98°N, 89.40°E; southern BoB), and station MONO6 (18.05°N, 89.38°E - northern BoB; Fig. 4).

The distribution of the PF average concentrations across different depth intervals shows that highest values occur within the upper 40 metres of the water column (Fig. 4). At MONO1 and MONO9, absolute abundances are ~10 ind/m^3 and ~40 ind/m^3 in the 0-20 m depth interval, respectively. Station MONO6, the northernmost station, differs from the others in that the PF absolute abundance is relatively high in the upper 20 m (~7 ind/m^3), and then relatively stable between ~2 and 4 ind/m^3 with depth (20-40 m, 40-60 m, 60-80 m, and 80-100 m). MONO4 contains very few specimens in the 0-20 m depth interval (~1 ind/m^3) and slightly more in the depth interval 20-40 and 40-60 m (3 ind/m^3).

4.4.2. Depth habitat of planktonic foraminifera

The DH allows us to estimate a mean dwelling depth of the different species and allows us to compare our results to other plankton tow studies (e.g. Rebotim et al., 2017; Lessa et al., 2020).

In the northern BoB, at station MONO6, the DHs and associated SE of *N. dutertrei*, *G. bulloides*, and *G. glutinata* are 86±29 m (VDR=60m), 98 ±39m (VDR=103m), and 153±46 m (VDR=137 m), respectively. These DHs are associated with broad vertical dispersion ranges (Fig. 4; Table 2). At the nearby station MONO4, *G. bulloides* (DH=91±33 m, VDR=87 m) and *N. dutertrei* (DH=57±24 m, VDR= 44 m) show deeper dwelling depths and wider vertical dispersion, though to a lesser extent than at MONO6. *Globigerinoides ruber* and *T. sacculifer* typically have DHs above 40 m at most stations. At the remaining stations, most species inhabit surface waters, with exceptions such as *G. cultrata* at station MONO9 (DH=70±14 m, VDR=27 m) and *G. glutinata* at stations MONO2 (central BoB; DH=64±26 m, VDR=57 m) and MONO1 (southern BoB; DH=68±26 m, VDR=57 m). On average, across the five stations and from the shallowest to the deepest habitats, *G. ruber* and *T. sacculifer* have the shallowest DHs (33±4 m and 34±11 m, respectively), followed by *N. dutertrei* (50±23), *G. bulloides* (32±39 m), *G. cultrata* (57±14 m), and *G. glutinata* (82±45 m) (Fig. 5; Table 2). Similarly, PF displays maximum absolute abundance distribution within

Table 4
Table listing the environmental (WOD, Boyer et al., 2018) and foraminiferal habitat data used for linear correlation analysis (Fig. 6) MLD: mixed layer depth; MLT: mixed layer temperature; MLS: mixed layer salinity; MLC: mixed layer chlorophyll-a concentration; TD: thermocline depth; DCM: deep chlorophyll maximum depth.

	Stations	MONO1	MONO2	MONO4	MONO6	MONO9
Environmental parameters	MLD (m)	40	23	34.9	25	35
	MLC (mg/L)	0.2	0.03	0.09	0.04	0.1
	TD (m)	83.5	131.2	129.2	162.9	127.2
	DCM depth (m)	49.5	60.7	70	65	80.8
	MLT (°C)	29.5	30	29.4	29.4	29.5
	MLS (psu)	33.5	32.9	33.0	33.0	33.3

the mixed layer apart from *N. dutertrei* and *G. cultrata* that display a bimodal pattern.

Across the MONOPOL stations, all species showed markedly non-normal vertical distributions, with skewness consistently deviating from zero and kurtosis generally strongly positive (Table 2). *Globigerinoides ruber* exhibited the most extreme patterns, with highly positive skewness (4.0–5.2) and very high kurtosis (19.2–36.8), indicating a high concentration in the surface- and sharply peaked distribution. *Trilobatus sacculifer* was more variable, with mostly positive skewness (2.2–5.2) and high kurtosis (5.8–42.9), but also one case of negative skewness (–3.5), reflecting a deeper-biased tail at MONO4. *Neogloboquadrina dutertrei* and *G. bulloides* both maintained moderate positive skewness (0.9–3.9) and positive kurtosis, though kurtosis values ranged from nearly uniform (-1.0) to sharply peaked (>20). *G. cultrata* also showed mostly positive skewness (2.3–5.5) with a single negative case (-1.4 at MONO6), and kurtosis ranging between 2.3 and 32.6. In contrast, *G. glutinata* exhibited the broadest variability: skewness ranged from near-symmetry (0.0 at MONO6) to moderately positive (up to 3.9), while kurtosis spanned from negative (–2.0 at MONO6) to very high (23.8 at MONO9), suggesting alternation between flat, widely spread distributions and highly peaked surface-concentrations.

4.4.3. Linear correlation analysis

The linear correlation analysis provides insight into the relationships between environmental factors and depth habitat distribution of key PF species depicted by DH, VDR, skewness and kurtosis metrics. Only a few significant correlations were detected (Fig. 6). For *G. bulloides,* the depth of maximum concentration is strongly and positively correlated with the MLD. However, *G. bulloides* shows concentration of less than 5 ind/m^3 at 3 stations, which could be too low to obtain robust correlation results. For *N. dutertrei*, DH is significantly and positively correlated with DCM depth, while the skewness of its vertical distribution is significantly and negatively correlated to the DCM depth.

5. Discussion

5.1. Modern planktonic foraminifera distribution across the Bay of Bengal

We find that modern PF assemblages in the BoB are dominated by six species, namely, *N. dutertrei*, *G. ruber*, *T. sacculifer, G. cultrata, G. glutinata* and *G. bulloides*. *N. dutertrei*, *G. ruber*, *T. sacculifer* and *G. cultrata* are tropical to subtropical species (e.g. Boltovskoy, 1969; Bé and Hutson, 1977; Bé and Tolderlund, 1971). *Globigerinita glutinata* is a cosmopolitan species, and *G. bulloides* is a species that generally dwells in the middle to high latitudes and in upwelling regions (Table 1; Bé and Hutson, 1977; Bé and Tolderlund, 1971; Kleijne et al., 1989; Zhang, 1985). Although these species are found in all samples, their relative abundances vary spatially. The data used to assess the spatial distribution of the six main planktonic foraminiferal species were quality checked to account for heterogenous sampling effort and methodological biases (cf. Section 3.1.4; Fig. 2B). The remaining plankton net data used in the ecological interpretations were collected during spring and summer (Osiris, MONOPOL, and sediment trap data). To ensure that the results of our analysis are directly applicable to fossil assemblages, we relied on relative rather than absolute abundances. This approach associated with the use of sediment trap fluxes and relative abundances recovered over multiple years in the BoB allows assessment of the general character of the PF community structure that facilitates broader comparisons. Flux data from Maeda et al., 2022 confirm that the main species targeted by our study are present year-round, with abundance peaks during the summer and winter monsoon and are usually highly correlated with periods of productivity peaks in the BoB. In view of these considerations, we believe our interpretation of the spatial distribution based on this compiled dataset is reasonable, and the results offer valuable and meaningful ecological insights.

Globigerinoides ruber and *T. sacculifer* exhibit distinct spatial distributions in the BoB, where *G. ruber* is prevalent in the warm, oligotrophic waters of the central BoB. In contrast, *T. sacculifer* is slightly more abundant at the southern tip of India and in the northern BoB (Fig. 3), where oceanographic conditions are influenced by upwelling associated to the southwest (boreal summer) monsoon (Narayanan Nampoothiri et al., 2020) and the Ganges-Brahmaputra river plume, which reaches maximum freshwater discharges from June to October (Papa et al., 2010). Surface sediment data from the western BoB margin (Bhadra and Saraswat, 2021) support this finding, showing that *G. ruber* dominates in waters with salinities higher than 32 but declines considerably in fresher environments near river mouths, where *T. sacculifer* "without sac" is more common. Along this line of observations, in the NBBT sediment trap (Guptha et al., 1997; Fig. 3), *G. ruber* features lower fluxes than *T. sacculifer* during summer months of maximum monsoon-fuelled river discharge in the northern BoB (Fig. 3). These results collectively indicate that *G. ruber* and *T. sacculifer* despite occupying similar ecological niches, tenuous variation in the plankton composition on which they feed can favour one species over the other (Table 4; Bé and Hutson, 1977; Ufkes et al., 1998; Maeda et al., 2022).

Both *G. ruber* and *T. sacculifer* are symbiont-bearing (usually dinoflagellates) mixed-layer species that generally prefer oligotrophic waters (e.g., Ravelo et al., 1990; Ravelo and Andreasen, 1999; Siccha and Kucera, 2017; Morard et al., 2019; Takagi et al., 2019) and tolerate wide ranges of temperature and especially salinity (e.g., Thunell and Reynolds, 1984; Bijma et al., 1990b; Hilbrecht, 1997). Yet, regional specificities for these species have been documented, such as the inverse spatial relationship between *T. sacculifer* and *G. ruber* also in other parts of the Indian Ocean (Bé and Hutson, 1977), albeit it contrasts with the pattern observed in the BoB. In the Caribbean and tropical Atlantic Ocean (Schmuker, 2000; Schmuker and Schiebel, 2002; Ufkes et al., 1998), *T. sacculifer* and *G. ruber* occur in high abundances, with *G. ruber* prevailing in the low-salinity water lenses that originate from the Amazon and Orinoco Rivers (Schmuker, 2000; Schmuker and Schiebel, 2002). In the tropical eastern Atlantic, *G. ruber* and *T. sacculifer* dominate coastal assemblages, with *G. ruber ruber* (pink chromotype; Morard et al., 2019) being more abundant in the low-salinity Congo river plume (Ufkes et al., 1998). Similarly, *G. ruber* dominates the PF assemblages in the eastern Mediterranean Sea during sapropel events (e.g., Corselli et al., 2002; Mojtahid et al., 2014), which suggests its adaptation to considerable surface freshening tied to enhanced, monsoon-fuelled North African runoff (e.g., Rohling et al., 2004; Rodríguez-Sanz et al., 2017; Amies et al., 2019). Similar regional differences in the distribution of *G. ruber* and *T. sacculifer* have been reported before (e.g., Bijma et al., 1990b), calling for detailed assessments of their distribution in basins of the world's ocean where environmental controlling factors are distinct. The euryhaline nature of both *G. ruber* and *T. sacculifer* (Bijma et al., 1990b) suggests that their spatial distributions in the BoB are unlikely driven by the steep and seasonally variable salinity gradients of the region (Hood et al., 2024). Enhanced turbidity near the major river plumes of the BoB is also unlikely to be the primary factor controlling the observed distinct spatial distributions of *G. ruber and T. sacculifer*. Since both species harbour algal symbionts (Gastrich, 1987; Takagi et al., 2019), they would respond similarly to turbidity induced reductions in light penetration in the upper water column. Therefore, we argue that species-specific dietary preferences play a role in spatial distributions of *G. ruber* and *T. sacculifer* that we find in the BoB. *G. ruber*'s tolerance to oligotrophic conditions likely reflects its capacity to feed on various phytoplankton groups (opportunistic behaviour, e.g., Schiebel and Hemleben, 2017). In contrast, *T. sacculifer* is more specialised, preferring specific prey such as calanoid copepod (Hemleben et al., 1989), which are more abundant in the nutrient-rich water in the vicinity of river mouths (Arunpandi et al., 2022). Furthermore, CBBT sediment trap data show that the fluxes and relative abundances of these two species peak at different months of the year: May for *G. ruber* and June for *T. sacculifer* (Fig. 3; Maeda et al., 2022a). Maeda et al., 2022a explain this species

temporal succession in the BoB by the ability of *G. ruber* to feed on phytoplankton, which allows it to flourish during the initial phase of trophic chain formation at the surface, whereas *T. sacculifer* becomes more prominent later, as zooplankton populations develop. Finally, we could gain further insights into the ecological preferences of *G. ruber* in the BoB by characterising the spatial distributions of *G. ruber albus* and *G. elongatus*, as in the nearby Arabian Sea they preferentially dwell in oligotrophic and eutrophic conditions, respectively (Seears et al., 2012).

Neogloboquadrina dutertrei dominates the assemblages with relative abundances of ~50% around the southern tip of India and in the proximity of the Ganges-Brahmaputra River system in the north (Fig. 3). In the Indian Ocean, *N. dutertrei* generally occurs in the proximity of oceanic fronts and boundary currents (Bé and Hutson, 1977; Boltovskoy, 1969), and in areas influenced by the WMC (Fig. 1; Belyaeva, 1964; Bé and Hutson, 1977) that flows at ~5°N transporting low-salinity waters from the BoB towards the eastern Arabian Sea (Shankar et al., 2002). This association between WMC and *N. dutertrei* has been used to explain the high abundance of this species in the surface sediments of the southeastern Arabian Sea (Naidu, 1993). The high abundances of *N. dutertrei* in the sector of the BoB influenced by the Ganges-Brahmaputra River plume (Fig. 3) and, more generally, in the northern BoB (Cullen, 1981) lends support to the notion that *N. dutertrei* is a low-salinity indicator (Bé and Tolderlund, 1971; Cullen, 1981; Ufkes et al., 1998). This is further exemplified by its occurrence in the low-salinity Congo river plume (Ufkes et al., 1998) and in downcore records of enhanced freshwater input from the Gulf of Mexico (Kennett and Shackleton, 1975; Thunell, 1976) and the Mediterranean Sea (Thunell et al., 1977; Thunell, 1978). On the other hand, core-top observations in the western BoB margin (Bhadra and Saraswat, 2021) suggest that there is no direct link between *N. dutertrei* abundances and surface waters salinity conditions. Moreover, the early-summer peak of the *N. dutertrei* fluxes and relative abundances in the NBBT and CBBT sediment traps (Fig. 3) has been linked to water column stratification and the development of a distinct DCM at the top of the thermocline (Guptha et al., 1997; Stoll et al., 2007; Maeda et al., 2022). During the southwest monsoon season, haline stratification develops in response to enhanced freshwater discharge from the Ganges-Brahmaputra River system (Thadathil et al., 2007). Combined with a positive wind-stress curl, this causes both mixed layer depth and thermocline to shoal in the northern BoB, thereby increasing chlorophyll concentrations within the DCM (Chowdhury et al., 2021). Our analysis also reveals the high abundances of *N. dutertrei* near the southern tip of India (Fig. 3), a region characterised by upwelling during the boreal summer monsoon season, which coincides with the deployment of the OSIRIS II plankton nets (Duplessy et al., 1981; Zhang, 1985). This evidence agrees with the occurrence of *N. dutertrei* in other highly productive upwelling systems, such as in the eastern Pacific Ocean (Fairbanks et al., 1982) and in the western Arabian Sea (Cullen, 1981; Bé and Hutson, 1977). The Arabian Sea features salinities that are considerably higher than in the BoB (Hood et al., 2024), and it shows that *N. dutertrei* is rather indifferent to salinity changes and not exclusively tied to low salinity environments.

To conclude, in the BoB, *N. dutertrei* thrives in highly stratified waters in the northern sector of the BoB that are associated with a distinct DCM, and in nutrient-rich upwelling systems off the southern tip of India. Its distribution is mainly modulated by food availability instead of other environmental parameters like salinity. In the southern and central BoB, lower relative *N. dutertrei* abundances may result from greater species diversity, including other dominant planktonic foraminifera, such as *G. ruber*.

Likewise, *N. dutertrei, G. bulloides* is also abundant (>20%) near the southern tip of India, but it is conspicuously less present (<5%) along the 90°E transect in the centre of the BoB (Fig. 3). Previously, *G. bulloides* has been associated with middle to high latitude cold waters and/or upwelling nutrient-rich environments at lower latitudes (Bé and Hutson, 1977; Bé and Tolderlund, 1971; Kleijne et al., 1989; Zhang, 1985). This agrees with its spatial distribution across the Indian Ocean (Bé and Hutson, 1977), where *G. bulloides* abounds in the upwelling systems of the western Arabian Sea, the southern tip of India, and the eastern coast of India (Cullen and Prell, 1984; Duplessy et al., 1981; Zhang, 1985; Bhadra and Saraswat, 2021). In the northernmost and southernmost BoB sediment traps (NBBT, SBBT), *G. bulloides* fluxes indicate peaks during the SW (boreal summer) monsoon season and features another lower peak abundance during the NE (boreal winter) monsoon. In the central BoB (CBBT), the only significant peak occurs during the SW monsoon (Guptha and Mohan, 1996; Guptha et al., 1997; Fig. 3). Fluxes at SBBT are about twofold higher during the peak summer monsoon than at NBBT and CBBT (Guptha and Mohan, 1996), because this sector may experience higher productivity due to open-ocean upwelling (Vinayachandran et al., 2005). Conversely, northern sites may experience enhanced nutrient-rich river discharge, but the associated reduction in surface-water salinity may be unfavourable to *G. bulloides*. Overall, *G. bulloides* seems closely linked to highly productive environments in the BoB upwelling systems and does not tolerate low salinities.

Globigerinita glutinata and *G. cultrata* exhibit similar spatial distributions in the BoB (Fig. 3), with two key patterns: i) *G. glutinata* show a subtle presence near the southern tip of India, where summer monsoon driven upwelling occurs (Duplessy et al., 1981; Schott and McCreary Jr., 2001; Vinayachandran et al., 2021). This agrees with *G. glutinata*'s known association with low-latitude upwelling systems, mid-latitude seasonal phytoplankton (diatom) blooms (Schiebel et al., 2001), and localised phytoplankton blooms in cyclonic eddies (e.g., in the Caribbean; Schmuker and Schiebel, 2002).

Globorotalia cultrata exhibits low occurrences at the southern tip of India, aligning with the findings of Bé and Hutson (1977) in the same region. This contrasts with its high abundances in the equatorial and the upwelling regions of the western (off Somalia, Yemen, and Oman) and eastern Arabian Sea (near the southern tip of India), and in the central western BoB (Bé and Hutson, 1977). The inconsistent association of this species with Indian Ocean upwelling systems suggests that other water column properties or morphotype differentiation may play a role (Adelseck, 1975; Bé and Hutson, 1977). Alternatively, high *G. cultrata* abundances near the western part of the tip of India may be linked to westward WMC advection (Naidu, 1993), which was absent during the OSIRIS II cruise (July; Duplessy et al., 1981). Indeed, *G. cultrata* is associated with strong ocean currents, specifically the Gulf Stream and the Brazil Current in the Atlantic (Bé and Tolderlund, 1971) and the reappearance of *G. cultrata* in the Atlantic during the Holocene is linked to the deglacial strengthening of the Agulhas leakage (e.g., Peeters et al., 2004; Marino et al., 2013; Broecker and Pena, 2014).

(ii) Both species are more abundant in the northern BoB stations that are more directly influenced by the freshwater discharges of the Ganges-Brahmaputra River. *Globigerinita glutinata* is known to thrive in both highly saline Arabian Sea waters and low-salinity water of the northern BoB (Cullen, 1981), indicating perhaps a broad salinity tolerance. Alternatively, its distribution may not be directly driven by salinity but rather by co-varying factors such as nutrient availability, to which it responds opportunistically. However, for *G. cultrata,* its distribution (Fig. 3) contradicts the study of Cullen and Prell (1984) that reported increasing abundance southward in the BoB with rising temperature and salinity. A shallower lysocline in the northern BoB may bias results by dissolving *G. cultrata* tests (Cullen and Prell, 1984). While typically linked to high-temperature waters (Kennett and Huddlestun, 1972; Balsam and Flessa, 1978; Naidu, 1991; Huang et al., 2003), no evidence suggests that *G. cultrata* tolerates low salinity. Given its link to strong currents identified by Bé and Tolderlund (1971) and Naidu (1993), its northern BoB abundance may be influenced by the dynamics of the EICC, which flows through these stations in spring and intensifies in summer (Fig. 1).

Further insights into the ecological requirements of the six major species may be gained by examining their vertical distribution in the water column (see Section 5.2).

5.2. Vertical distribution of the major planktonic foraminiferal species

The vertical habitat of PF is determined in the central BoB along a north-south transect of the five MONOPOL stations (Fig. 2), which were sampled in May–June 2012 (Fig. 2; Table 1), i.e., towards the end of the pre-monsoon season and at the very beginning of the summer monsoon season (Hood et al., 2024). Depth habitat for each species is expressed in terms of absolute abundances, DH, VDR (Fig. 4; Fig. 5), following Rebotim et al. (2017) and Lessa et al. (2020).

During the sampling season, the mixed layer salinity and temperature show subtle variations across stations (Fig. 4; Table 4), making them unlikely drivers of the observed different PF vertical distributions among species. The relatively uniform north-south surface salinity distribution results from the southward redistribution of low-salinity water, driven by northeasterly winds, the equatorward EICC, and the westward WMC during the preceding fall and winter (Akhil et al., 2014). This setting thereby weakens the strong meridional salinity gradient that develops during the southwest monsoon season (Vinayachandran et al., 1999; Shankar et al., 2002; Fournier et al., 2017). Despite surface salinity uniformity, studies show that the northern BoB's upper water column remains stratified throughout the summer monsoon (e.g., Chowdhury et al., 2021; Chaitanya et al., 2021). In contrast, the southern BoB's stratification is disrupted during summer by monsoon winds and high salinity water from the Arabian Sea advected via the SMC (Narvekar and Prasanna Kumar, 2014; Prasanth et al., 2023). This upper water column structure affects PF distribution by controlling surface or subsurface primary productivity (Stoll et al., 2007; Maeda et al., 2022).

Globally, the vertical distribution of PF is primarily influenced by temperature, salinity, primary productivity, light saturation, food, oxygen, and nutrients availability, as well as water column stratification (e.g., Fairbanks et al., 1982; Schiebel et al., 2001; Field et al., 2006; Kuroyanagi and Kawahata, 2004; Salmon et al., 2015; Rebotim et al., 2017). Other biological factors have been also reported such as ontogeny across a lunar cycle, with contradictory evidence of migration and descent preceding gamete release during sexual reproduction close to full moon (Bijma et al., 1990a; Jonkers et al., 2015, Jonkers et al., 2017; Meilland et al., 2021).

Considering the temperature and salinity patterns discussed above and the oceanographic setting of the BoB (Hood et al., 2024) during the sampling period, we perform a multiple correlation analysis. The statistically not significant correlations observed between the tested environmental factors (Table 3; Fig. 6) and depth distribution parameters for some species (Fig. 6) may stem from: (i) the relatively small sample size (only five stations), or (ii) the subtle variability of the environmental factors across the basin at this time of the year which we may have smoothed out by averaging environmental data, and/or (iii) the influence of additional factors that have yet to be identified (e.g., biotic processes, such as species interactions, reproductive timing, or patchiness; e.g., Meilland et al., 2021).

When considering all PF species together, we find that most of the standing stock is concentrated within the mixed layer (Fig. 5). At the northernmost station MONO6, the DHs are deeper and the VDRs are broader than at other stations (Fig. 4), most likely due to unique environmental conditions of this sector of the BoB. In our analysis, MONO6 is distinct from the other stations due to the deepest thermocline (Fig. 4). The thermocline is a key gradient zone for several key parameters other than temperature itself (e.g., temperature, nutrient availability, oxygen), and a deeper thermocline can shift the depth habitat of PF species (e.g., Fairbanks et al., 1980). When examining the six dominant species individually, the vertical distribution of some species appears consistent across the MONOPOL stations, while others occupy different depths of the water column (Fig. 4), which we interpret as the PF response to changing depth of certain environmental features across the BoB.

Globigerinoides ruber and *T. sacculifer* consistently inhabit depths above ~40 m across the north-south MONOPOL transect during May–June and reside within the mixed layer or near the MLD (Fig. 4; Fig. 5). This depth preference is similar to their overall DH across the Indian Ocean (respectively, 39.43±2.07 m and 34.97±1.87 m; Chaabane et al., 2025), in the subtropical eastern North Atlantic and subtropical South Atlantic (<50 m; Rebotim et al., 2017; Lessa et al., 2020). In the central equatorial Pacific and southeast Atlantic, *G. ruber* (white) is also found in the upper 50–60 m (Watkins et al., 1996; Kemle-von Mücke and Oberhänsli, 1999), while in the Azores Front-Current System, it is most abundant in the upper 100 m (Schiebel, 2002). Using stable isotopes and Mg/Ca ratios on core top samples from the northern equatorial Indian Ocean, Stainbank et al. (2019) found that *G. ruber* and *T. sacculifer* typically calcify within the mixed layer. Similarly (Maeda et al., 2022) analysed multiyear sediment-trap samples from the central BoB (CBBT) and reported that *G. ruber* predominantly calcifies in the surface mixed layer, while *T. sacculifer* calcifies slightly deeper. Both *G. ruber* and *T. sacculifer* are photosymbiont-bearing species (Hemleben et al., 1989; Takagi et al., 2019), which likely explains their high abundance in the light-saturated uppermost water column and narrow living depth range (Spero and Lea, 1993; Chaabane et al., 2025). Consistency of their depth preferences across the BoB during May–June, along with evidence from other ocean basins, collectively suggests that these species are valuable geochemical signal carriers to reconstruct changes in mixed layer properties. Their constraint habitat in the surface layer is essential for accurately linking their geochemical signals (e.g., stable isotopes, trace elements) to environmental properties at those depths, thereby capturing the variability in the surface on past climate records. One caveat is that *T. sacculifer* may add gametogenic calcite while reproducing at deeper depth (~80 m; Duplessy et al., 1981; Stainbank et al., 2019), which could explain the deeper calcification depth calculated by Maeda et al., 2022 in sediment trap data. This process was not captured in our dataset, unless we hypothesise that the fewer individuals found in the deeper interval of the nets were dead sinking *T. sacculifer* after reproduction. Also, no distinction was made between *T. sacculifer* morphotypes (with or without sac-like final chamber), which would provide important information for the selection of *T. sacculifer* specimens in palaeoceanographic reconstructions based on shell geochemistry.

We find that *N. dutertrei* reaches its highest absolute abundances within and at the base of the mixed layer at all MONOPOL stations (Fig. 5), consistent with plankton tow observations from the wider Indian Ocean (Chaabane et al., 2025), and from the subtropical northeast Atlantic (Rebotim et al., 2017). Individuals of this species are also found at greater depths, particularly at the northernmost station, MONO6. At this site, this species features a DH of 87±29m and a VDR of ~60 m (Table 2), which correspond to the DCM and the upper thermocline (Fig. 4; Fig. 6; Tableau 4). Specimens collected near the DCM likely reflect the development of a subsurface trophic chain (Stoll et al., 2007; Maeda et al., 2022). In contrast, those found in the deepest net intervals (180–400 m) probably represent dead, sinking shells from individuals that reproduced at depth near the full moon (Meilland et al., 2021).

These results collectively suggest that *N. dutertrei* can inhabit both surface and deeper waters. This adaptability may be linked to its (facultative) symbiotic relationship with *Pelagophyceae*, which thrives in conditions of relatively low light intensity (Takagi et al., 2019), allowing *N. dutertrei* to live in the subsurface. Since the pioneering studies by Fairbanks et al. (1982) and Watkins et al. (1996), *N. dutertrei* has been widely recognised as a typical thermocline species associated with the DCM, which would agree with the evidence from MONO6 and the position of the DCM in May–June (Chowdhury et al., 2021), associated to the stratified environment of the northern BoB. Indian Ocean core-top data also indicate that *N. dutertrei* primarily calcifies within the thermocline (Cayre and Bassinot, 1998), a pattern supported by sediment-trap data from the central BoB (Maeda et al., 2022) and plankton net studies in the western Pacific warm pool (Rippert et al., 2016). Accordingly, this species has been widely used to reconstruct subsurface water conditions (Spero and Lea, 2002; Mohtadi et al., 2010; Bolton

et al., 2013; Davis, 2022), assuming a constant depth habitat within the thermocline (e.g., Umling and Thunell, 2017; Khan et al., 2023; Sánchez and Carriquiry, 2024).

A stable oxygen and carbon isotope study on the individual chambers of *N. dutertrei* from plankton net samples documents the vertical migration of this species through ontogeny (Takagi et al., 2016). MONOPOL samples have been collected over a three-week sampling campaign in May and June, which may not comprehensively document ontogenic depth migration of this species. Additionally, secondary calcite encrustation in colder waters could affect the oxygen isotope values of foraminiferal shells, potentially integrating calcification depth estimates toward deeper waters (Jonkers et al., 2012; Rebotim et al., 2017). Hence our analysis provides a first-order estimate of some aspects of ecological preferences and depth distribution of *N. dutertrei* across the BoB, which calls for a region-specific assessment of the dwelling and calcification depths for this species in other seasons, given the strong salinity fluctuations and highly variable DCM and thermocline depths in the BoB.

Globigerina bulloides generally shows low occurrence or is absent in the central BoB (MONOPOL stations). This may be due to unfavourable hydrographic conditions, such as low surface salinity (~33; Fig. 4) and oligotrophic conditions during the sampling period. This pattern is further supported by sediment trap data from Guptha and Mohan (1996), which show low flux and relative abundances of *G. bulloides* during May–June (Fig. 3r). Our analysis reveals that the highest absolute abundances of this species are generally found in the mixed layer (Fig. 4). At the northernmost station (MONO6), a few specimens are observed deeper in the water column, which explains the deep average living depth (DH) of ~97 m (Table 2). *Globigerina bulloides* is generally considered as a surface dweller restricted to the upper ~100 m of the water column (e.g., Bé and Hamlin, 1967; van Raden et al., 2011), although some studies document deeper habitats (e.g., Schiebel et al., 2001; Wilke et al., 2009; Rebotim et al., 2017). Rebotim et al. (2017) suggest that this species may occupy a broader vertical niche due to the lack of symbionts, which makes it independent of light saturation. Mortyn and Charles (2003) reported that this species inhabits varying depths in the Southern Ocean, with abundance and shell chemistry potentially influenced by density horizons, which are more pronounced than in the BoB. This broad vertical distribution is also reflected in the estimated calcification depths reported in several studies using oxygen isotopic composition, ranging from the shallow mixed layer to below the thermocline (e.g., Saraswat and Khare, 2010). The temporally limited sampling coverage of of the MONOPOL data set, along with the low occurrence of *G. bulloides* during May–June and its variable depth habitat hinder a sound assessment of the water column parameter(s) influencing the depth distribution of *G. bulloides* across the BoB. The tight link of *G. bulloides* to highly productive conditions and food availability, emphasises the need of studying its vertical distribution during the summer monsoon, the peak productive season in the BoB.

Globorotalia cultrata (formerly *G. menardii*) has an DH of approximately 40–70 m, with a relatively narrow VDR of ~12–32 m (Fig. 4). The depth of its maximum abundances aligns well with its DH, indicating that it consistently inhabits deeper waters than *G. ruber*, *T. sacculifer*, *N. dutertrei* and *G. bulloides* across all MONOPOL stations (Fig. 4; Fig. 5). During the pre-monsoon season in the BoB, a habitat depth of 40-70 m is below the mixed layer (Dandapat et al., 2021), coinciding with the DCM and the upper part of the thermocline (Fig. 4). This depth range is consistent with its mean calcification depth (51–83 m) in the South China Sea, where it corresponds to the seasonal thermocline or the deep mixed layer (Regenberg et al., 2010). Similar observations off Indonesia place it just below the lower boundary of the mixed layer (DH = 67-87 m; Tapia et al., 2022). In the western tropical Pacific, *G. cultrata* migrates between the uppermost thermocline during the day and the surface mixed layer at night (Ko et al., 2025). In the southeast Atlantic, *G. cultrata* is concentrated at 50–100 m, associated with the Equatorial Undercurrent (Kemle-von Mücke and Oberhänsli, 1999), while in the subtropical South Atlantic, it inhabits depths of 30–40 m (VDR = 20–30 m) and was referred to as a mixed layer species (Lessa et al., 2020). Considering its consistent depth habitat across MONOPOL stations and its general alignment with previous studies, *G. cultrata* appears to be a potential indicator of the DCM and upper thermocline in the BoB. This well constrained habitat may aid in reconstructing palaeoceanographic changes by providing a consistent picture of the thermocline variability. Its use in concert with surface species like *G. ruber* or *T. sacculifer* could allow robust reconstruction of the upper water column variability that varies in step with local hydroclimate and broader oceanographic changes (e.g., Kumar et al., 2018).

Globigerinita glutinata exhibits the deepest DH (65-90 m) and the widest VDR (30-150 m) amongst all the six species, with its habitat spanning the deep mixed layer and the lower part of the thermocline in the BoB (Fig. 4; Fig. 5). This aligns with findings from the subtropical eastern North Atlantic (DH = 50-120 m; Rebotim et al., 2017), the seas around Japan (upper 200 m; Kuroyanagi and Kawahata, 2004), and some southeast Atlantic sites (deeper than 150 m; Kemle-von Mücke and Oberhänsli, 1999). It is also recorded at depths shallower than 100 m in the east North Atlantic (Schiebel et al., 2001), and between 0 and 120 m in the central equatorial Pacific (Watkins et al., 1996). The broad depth range of this species is probably because light availability does not influence its depth habitat since no algal symbionts are present. Consistent with previous studies, our findings suggest that *G. glutinata* occupies a range of ecological niches in the water column and may be influenced by environmental factors not fully captured in our analysis. Its broad depth range could limit its suitability for palaeoceanographic reconstructions that use stable isotopes for instance in the BoB.

6. Conclusions

To understand the spatial and vertical distribution of PF in the BoB, we analysed available data from plankton nets and sediment traps and discussed them in the context of the BoB oceanographic and productivity patterns. This helped define basin-specific ecological and environmental requirements and living depths of major PF species.

Our analysis highlights distinct characteristics of PF spatial and vertical distributions in the BoB compared to global trends:

(i) A distinct spatial relationship between mixed layer dwellers *G. ruber* and *T. sacculifer*: *G. ruber* thrives primarily in open ocean oligotrophic waters, while *T. sacculifer* prefers environments with zooplankton as a food source. We suggest this difference in the BoB is diet-driven, whereby *G. ruber*'s opportunistic feeding allows it to thrive in oligotrophic conditions, whereas *T. sacculifer* is more specialised and depends on a specific food source.

(ii) *N. dutertrei* is abundant in stratified waters near the Ganges-Brahmaputra River and in nutrient-rich upwelling zones off southern India. While globally considered a low-salinity indicator, its high abundance in the northern BoB appears linked and to the development of a productive DCM associated with a stratified water column. This is supported by its deep DH and associated positive correlation with DCM depth (Fig. 6), the high summer fluxes in this region. In the southern BoB, this species inhabits shallow habitats within the mixed layer in May–June, most likely caused by the weaker stratification that can easily be disrupted by winds, thereby injecting nutrient into the mixed layer.

(iii) *G. bulloides* follows known distribution patterns, occurring in productive upwelling regions. In the BoB, it typically has an DH shallower than ~60 m but is found deeper (~90 m) in northern waters. We suggest that this shift results from the deep thermocline.

(iv) *G. glutinata* and *G. cultrata* share similar spatial distributions in the BoB, with population minima near the southern tip of India, where upwelling occurs and maxima in the stratified northern

BoB stations. The low abundance of *G. cultrata* near southern India contrasts with its high presence in equatorial and upwelling regions of the Indian Ocean, suggesting its distribution is more influenced by ocean currents than upwelling alone. *Globorotalia cultrata* peaks at 50–70 m depth corresponding to the DCM and upper thermocline. *Globigerinita glutinata* has the deepest DH (65–90 m) and the broadest vertical range but remains below the mixed layer. These depth habitats align with global observations.

Given the limitations (e.g., limited number of samples) affecting our vertical distribution analysis, some tentative conclusions can be made about the species use as proxy carriers in palaeoceanography:

(i) *G. ruber* and *T. sacculifer* primarily inhabit the upper ~40 m in the BoB during May–June, aligning with observations from other oceanic regions. Their consistent depth preference makes them valuable geochemical indicators for reconstructing past mixed layer conditions.
(ii) Calcification depth estimates based on geochemical signatures typically link *N. dutertrei* to subsurface waters globally (e.g., Lakhani et al., 2022). In the BoB, its presence in the mixed layer during May–June suggests some habitat flexibility. This apparent difference may be due to seasonal oceanographic changes (e.g. stratification), lack of documentation of the full ontogenic depth migration, or secondary calcite encrustation. A better integration of these factors would improve its reliability as a proxy for paleoceanographic studies in the BoB.
(iii) *G. cultrata* consistently inhabits deeper waters, aligning with the DCM and the upper part of the thermocline, making it a potential palaeoceanographic indicator in the BoB. In contrast, *G. glutinata* has a broad depth habitat, which may limit its use as a reliable proxy-carrier.

7. Proposed directions for future research

We note that it is important to account for potential sources of bias in the interpretation of plankton tow data. These are unlikely to not overshadow the primary ecologically relevant signal, but may likely contribute to the variability in the data in some regions affected by strong seasonal changes in water column properties, like the BoB. For example, dead PF specimens may sink and be misclassified as living, and plankton tows provide only a brief snapshot in time and space (e.g., Rebotim et al., 2017). To address these limitations, we propose some research directions that are aimed at advancing our understanding of the PF distributions and ecological preferences and their use as geochemical signal carrier in palaeoceanography:

(i) Expanded sampling: Increasing spatial and time coverage will help clarify environmental influences on PF distributions in the BoB across seasonal and interannual timescales. This will be especially useful for species showing inconsistent depth habitats across the BoB.
(ii) Methodological refinements**:** Using a standard mesh size (100 μm) to capture small PF species, distinguishing living from dead cells, and integrating additional water column parameters (e.g., food type, oxygen levels, stable isotopes of carbon and oxygen) will improve our understanding of PF vertical distribution and environmental controls. Measuring geochemical elements in PF shells will also enhance calcification depth estimates and improve isotopic calibration for palaeoreconstructions.
(iii) Integrating biotic drivers into foraminiferal ecology: Greater emphasis should be placed on the role of biotic factors, such as species interactions, reproductive cycles, and population dynamics, in addition to physico-chemical variables, to achieve a more comprehensive understanding of the drivers shaping planktonic foraminiferal distribution.
(iv) Improved taxonomic identification: Applying molecular tools will allow for the identification of cryptic species, refining taxonomic classification and improving ecological interpretations.

CRediT authorship contribution statement

Rose Manceau: Writing – original draft, Methodology, Investigation, Formal analysis, Data curation, Conceptualization. **Meryem Mojtahid:** Writing – review & editing, Writing – original draft, Supervision, Investigation, Formal analysis. **Eelco Rohling:** Writing – review & editing. **Robin Fentimen:** Writing – review & editing. **Thibault de Garidel-Thoron:** Writing – review & editing. **Sonia Chaabane:** Writing – review & editing, Writing – original draft, Methodology, Data curation. **Gianluca Marino:** Writing – review & editing, Supervision.

Declaration of competing interest

The authors declare that they have no known competing financial interests or personal relationships that could have appeared to influence the work reported in this paper.

Data availability

Raw data is available on SEANOE data repository (https://doi.org/10.17882/104732)

Acknowledgments

We would like to thank N. Ministéri for the analysis of MONOPOL samples. We would like to thank Sonia Munir for providing data from Munir et al. (2022). We are grateful to Clara Bolton for the valuable discussions. Finally, we would like to thank Lukas Jonkers and an anonymous reviewer for their valuable comments and suggestions. This work was supported by the University of Angers.

Appendix A. Supplementary data

Supplementary data to this article can be found online at https://doi.org/10.1016/j.marmicro.2025.102518.

References

Adelseck, C.G., 1975. Living Globorotalia menardii (d'Orbigny) forma neoflexuosa from the eastern tropical Pacific Ocean. Deep-Sea Res. Oceanogr. Abstr. 22, 689–691. https://doi.org/10.1016/0011-7471(75)90007-8.
Ahmad, S.M., Zheng, H., Raza, W., Zhou, B., Lone, M.A., Raza, T., Suseela, G., 2012. Glacial to Holocene changes in the surface and deep waters of the northeast Indian Ocean. Mar. Geol. 329–331, 16–23. https://doi.org/10.1016/j.margeo.2012.10.002.
Akhil, V.P., Durand, F., Lengaigne, M., Vialard, J., Keerthi, M.G., Gopalakrishna, V.V., Deltel, C., Papa, F., de Montégut, C.B., 2014. A modeling study of the processes of surface salinity seasonal cycle in the Bay of Bengal. J. Geophys. Res. Oceans 119, 3926–3947. https://doi.org/10.1002/2013JC009632.
Amies, J.D., Rohling, E.J., Grant, K.M., Rodríguez-Sanz, L., Marino, G., 2019. Quantification of African monsoon runoff during last interglacial sapropel S5. Paleoceanogr. Paleoclimatol. 34, 1487–1516. https://doi.org/10.1029/2019PA003652.
Arunpandi, N., Jyothibabu, R., Jagadeesan, L., Lekshmi, S., Surya, S., Biju, A., 2022. Copepod carcasses in the western Bay of Bengal and associated ecology. Environ. Monit. Assess. 194, 137. https://doi.org/10.1007/s10661-021-09748-x.
Balsam, W.L., Flessa, K.W., 1978. Patterns of planktonic foraminiferal abundance and diversity in surface sediments of the western North Atlantic. Mar. Micropaleontol. 3, 279–294. https://doi.org/10.1016/0377-8398(78)90032-4.
Bassinot, F., Luc, Beaufort, 2012. MD 191/MONOPOL cruise. Marion Dufresne R/V. https://doi.org/10.17600/12200050.
Bé, A.W.H., Hamlin, W.H., 1967. Ecology of Recent Planktonic Foraminifera: Part 3: Distribution in the North Atlantic during the Summer of 1962. Micropaleontology 13, 87–106. https://doi.org/10.2307/1484808.
Bé, A.W.H., Hutson, W.H., 1977. Ecology of Planktonic Foraminifera and Biogeographic Patterns of Life and Fossil Assemblages in the Indian Ocean. Micropaleontology 23, 369–414. https://doi.org/10.2307/1485406.
Bé, A.W.H., Tolderlund, W.R., 1971. Distribution and ecology of living planktonic foraminifera in surface waters of the Atlantic and Indian Oceans. In: The Micropalaeontology of Oceans. Cambridge University Press.

Belyaeva, N.V., 1964. Distribution of planktonic foraminifera in the water and on the floor in the Indian Ocean. Okeanologia 68, 12–83.
Bergami, C., Capotondi, L., Langone, L., Giglio, F., Ravaioli, M., 2009. Distribution of living planktonic foraminifera in the Ross Sea and the Pacific sector of the Southern Ocean (Antarctica). Mar. Micropaleontol. 73, 37–48. https://doi.org/10.1016/j.marmicro.2009.06.007.
Bhadra, S.R., Saraswat, R., 2021. Assessing the effect of riverine discharge on planktic foraminifera: A case study from the marginal marine regions of the western Bay of Bengal. Deep Sea Research Part II: Topical Studies in Oceanography. In: The 2nd International Indian Ocean Expedition (IIOE-2): Motivating New Exploration in a Poorly Understood Basin (Volume 4), 183, 104927. https://doi.org/10.1016/j.dsr2.2021.104927.
Bijma, J., Erez, J., Hemleben, C., 1990a. Lunar and semi-lunar reproductive cycles in some spinose planktonic foraminifers. J. Foraminifer. Res. 20, 117–127.
Bijma, J., Faber, W.W., Hemleben, C., 1990b. Temperature and salinity limits for growth and survival of some planktonic foraminifers in laboratory cultures. J. Foraminifer. Res. 20, 95–116. https://doi.org/10.2113/gsjfr.20.2.95.
Bolton, C.T., Chang, L., Clemens, S.C., Kodama, K., Ikehara, M., Medina-Elizalde, M., Paterson, G.A., Roberts, A.P., Rohling, E.J., Yamamoto, Y., Zhao, X., 2013. A 500,000 year record of Indian summer monsoon dynamics recorded by eastern equatorial Indian Ocean upper water-column structure. Quat. Sci. Rev. 77, 167–180. https://doi.org/10.1016/j.quascirev.2013.07.031.
Bolton, C.T., Gray, E., Kuhnt, W., Holbourn, A.E., Lübbers, J., Grant, K., Tachikawa, K., Marino, G., Rohling, E.J., Sarr, A.-C., Andersen, N., 2022. Secular and orbital-scale variability of equatorial Indian Ocean summer monsoon winds during the late Miocene. Clim. Past 18, 713–738. https://doi.org/10.5194/cp-18-713-2022.
Boltovskoy, E., 1969. Living Planktonic Foraminifera at the 90°E Meridian from the Equator to the Antarctic. Micropaleontology 15, 237–255. https://doi.org/10.2307/1484923.
de Boyer Montégut, C., Madec, G., Fischer, A.S., Lazar, A., Iudicone, D., 2004. Mixed layer depth over the global ocean: An examination of profile data and a profile-based climatology. J. Geophys. Res. Oceans 109. https://doi.org/10.1029/2004JC002378.
Boyer, T.P., Baranova, O.K., Coleman, C., Garcia, H.E., Grodsky, A., Locarnini, R.A., Mishonov, A.V., Paver, C.R., Reagan, J.R., Seidov, D., Smolyar, I.V., Weathers, K.W., Zweng, M.M., 2018. World Ocean Database, p. 2018.
Broecker, W., Pena, L.D., 2014. Delayed Holocene reappearance of G. menardii. Paleoceanography 29, 291–295. https://doi.org/10.1002/2013PA002590.
Brummer, G.-J.A., Kučera, M., 2022. Taxonomic review of living planktonic foraminifera. J. Micropalaeontol. 41, 29–74. https://doi.org/10.5194/jm-41-29-2022.
Caron, D.A., Bé, A.W.H., Anderson, O.R., 1982. Effects of variations in light intensity on life processes of the planktonic foraminifer Globigerinoides sacculifer in laboratory culture. J. Mar. Biol. Assoc. U. K. 62, 435–451. https://doi.org/10.1017/S0025315400057374.
Casajus, N., Greco, M., Chaabane, S., Giraud, X., de Garidel-Thoron, T., 2025. _forcis: An R client to access the FORCIS database_. R package version 0.1.0.9000. https://frbcesab.github.io/forcis.
Cayre, O., Bassinot, F., 1998. Oxygen Isotope Composition of Planktonic Foraminiferal Shells over the Indian Ocean: Calibration to Modern Oceanographic Data. Mineral. Mag. 62A, 288–289. https://doi.org/10.1180/minmag.1998.62A.1.152.
Chaabane, S., de Garidel-Thoron, T., Giraud, X., Schiebel, R., Beaugrand, G., Brummer, G.-J., Casajus, N., Greco, M., Grigoratou, M., Howa, H., Jonkers, L., Kucera, M., Kuroyanagi, A., Meilland, J., Monteiro, F., Mortyn, G., Almogi-Labin, A., Asahi, H., Avnaim-Katav, S., Bassinot, F., Davis, C.V., Field, D.B., Hernández-Almeida, I., Herut, B., Hosie, G., Howard, W., Jentzen, A., Johns, D.G., Keigwin, L., Kitchener, J., Kohfeld, K.E., Lessa, D.V.O., Manno, C., Marchant, M., Ofstad, S., Ortiz, J.D., Post, A., Rigual-Hernandez, A., Rillo, M.C., Robinson, K., Sagawa, T., Sierro, F., Takahashi, K.T., Torfstein, A., Venancio, I., Yamasaki, M., Ziveri, P., 2023. The FORCIS database: A global census of planktonic Foraminifera from ocean waters. Sci. Data 10, 354. https://doi.org/10.1038/s41597-023-02264-2.
Chaabane, S., de Garidel-Thoron, T., Meilland, J., Sulpis, O., Chalk, T.B., Brummer, G.-J. A., Mortyn, P.G., Giraud, X., Howa, H., Casajus, N., Kuroyanagi, A., Beaugrand, G., Schiebel, R., 2024. Migrating is not enough for modern planktonic foraminifera in a changing ocean. Nature 1–7. https://doi.org/10.1038/s41586-024-08191-5.
Chaabane, S., Schiebel, R., Meilland, J., Brummer, G.-J.A., Mortyn, P.G., Sulpis, O., Chalk, T.B., Giraud, X., Howa, H., Kuroyanagi, A., Beaugrand, G., Garidel-Thoron, T. D., 2025. Reassessment of the Global Distribution and Diversity of Modern Planktonic foraminifera from the FORCIS Database. Pre-print.
Chaitanya, A.V.S., Vialard, J., Lengaigne, M., d'Ovidio, F., Riotte, J., Papa, F., James, R. A., 2021. Redistribution of riverine and rainfall freshwater by the Bay of Bengal circulation. Ocean Dyn. 71, 1113–1139. https://doi.org/10.1007/s10236-021-01486-5.
Chauhan, O.S., Vogelsang, E., 2006. Climate induced changes in the circulation and dispersal patterns of the fluvial sources during late Quaternary in the middle Bengal Fan. J. Earth Syst. Sci. 115, 379–386. https://doi.org/10.1007/BF02702050.
Chauhan, O.S., Patil, S.K., Suneethi, J., 2004. Fluvial influx and weathering history of the Himalayas since Last Glacial Maxima – isotopic, sedimentological and magnetic records from the Bay of Bengal. Curr. Sci. 87, 509–515.
Chowdhury, K.M.A., Jiang, W., Liu, G., Ahmed, Md.K., Akhter, S., 2021. Dominant physical-biogeochemical drivers for the seasonal variations in the surface chlorophyll-a and subsurface chlorophyll-a maximum in the Bay of Bengal. Reg. Stud. Mar. Sci. 48, 102022. https://doi.org/10.1016/j.rsma.2021.102022.
Clemens, S.C., Yamamoto, M., Thirumalai, K., Giosan, L., Richey, J.N., Nilsson-Kerr, K., Rosenthal, Y., Anand, P., McGrath, S.M., 2021. Remote and local drivers of Pleistocene South Asian summer monsoon precipitation: A test for future predictions. Sci. Adv. 7, eabg3848. https://doi.org/10.1126/sciadv.abg3848.
Corselli, C., Principato, M.S., Maffioli, P., Crudeli, D., 2002. Changes in planktonic assemblages during sapropel S5 deposition: Evidence from Urania Basin area, eastern Mediterranean. Paleoceanography 17, 1–30. https://doi.org/10.1029/2000PA000536.
Cullen, J.L., 1981. Microfossil evidence for changing salinity patterns in the Bay of Bengal over the last 20 000 years. Palaeogeogr. Palaeoclimatol. Palaeoecol. 35, 315–356. https://doi.org/10.1016/0031-0182(81)90101-2.
Cullen, J.L., Prell, W.L., 1984. Planktonic foraminifera of the northern Indian Ocean: Distribution and preservation in surface sediments. Mar. Micropaleontol. 9, 1–52. https://doi.org/10.1016/0377-8398(84)90022-7.
Dandapat, S., Chakraborty, A., Kuttippurath, J., Bhagawati, C., Sen, R., 2021. A numerical study on the role of atmospheric forcing on mixed layer depth variability in the Bay of Bengal using a regional ocean model. Ocean Dyn. 71, 963–979. https://doi.org/10.1007/s10236-021-01475-8.
Davis, C.V., 2022. Deglacial restructuring of the Eastern equatorial Pacific oxygen minimum zone. Commun. Earth Environ. 3, 1–8. https://doi.org/10.1038/s43247-022-00477-8.
de Garidel-Thoron, T., Chaabane, S., Giraud, X., Meilland, J., Jonkers, L., Kucera, M., Brummer, G.-J.A., Grigoratou, M., Monteiro, F.M., Greco, M., Mortyn, P.G., Kuroyanagi, A., Howa, H., Beaugrand, G., Schiebel, R., 2022. The foraminiferal response to climate stressors project: tracking the community response of planktonic foraminifera to historical climate change. Front. Mar. Sci. 9. https://doi.org/10.3389/fmars.2022.827962.
d'Orbigny, A., 1826. Tableau Méthodique de la classe des Céphalopodes. Annales des Sciences Naturelles 7 (96–169), 245–314.
Ding, Y., Li, C., Liu, Y., 2004. Overview of the South China Sea monsoon experiment. Adv. Atmos. Sci. 21, 343–360.
Duplessy, J.C., Bé, A.W.H., Blanc, P.L., 1981. Oxygen and carbon isotopic composition and biogeographic distribution of planktonic foraminifera in the Indian Ocean. Palaeogeogr. Palaeoclimatol. Palaeoecol. Oxygen Carbon Isotopes Foraminifera 33, 9–46. https://doi.org/10.1016/0031-0182(81)90031-6.
Emiliani, C., 1955. Pleistocene temperatures. J. Geol. 63, 538–578. https://doi.org/10.1086/626295.
Erez, J., Almogi-Labin, A., Avraham, S., 1991. On the Life History of Planktonic Foraminifera: Lunar Reproduction Cycle in Globigerinoides Sacculifer (Brady). Paleoceanography 6, 295–306. https://doi.org/10.1029/90PA02731.
Fairbanks, R.G., Wiebe, P.H., 1980. Foraminifera and chlorophyll maximum: vertical distribution, seasonal succession, and paleoceanographic significance. Science 209, 1524–1526. https://doi.org/10.1126/science.209.4464.1524.
Fairbanks, R.G., Wiebe, P.H., Bé, A.W.H., 1980. Vertical distribution and isotopic composition of living planktonic foraminifera in the western north atlantic. Science 207, 61–63. https://doi.org/10.1126/science.207.4426.61.
Fairbanks, R.G., Sverdlove, M., Free, R., Wiebe, P.H., Bé, A.W.H., 1982. Vertical distribution and isotopic fractionation of living planktonic foraminifera from the Panama Basin. Nature 298, 841–844. https://doi.org/10.1038/298841a0.
Field, D.B., Baumgartner, T.R., Charles, C.D., Ferreira-Bartrina, V., Ohman, M.D., 2006. Planktonic foraminifera of the california current reflect 20th-century warming. Science 311, 63–66. https://doi.org/10.1126/science.1116220.
Fournier, S., Vialard, J., Lengaigne, M., Lee, T., Gierach, M.M., Chaitanya, A.V.S., 2017. Modulation of the ganges-brahmaputra river plume by the indian ocean dipole and eddies inferred from satellite observations. J. Geophys. Res. Oceans 122, 9591–9604. https://doi.org/10.1002/2017JC013333.
Gastrich, M.D., 1987. Ultrastructure of a new intracellular symbiotic alga found within planktonic foraminifera. J. Phycol. 23, 623–632. https://doi.org/10.1111/j.1529-8817.1987.tb04215.x.
Girishkumar, M.S., Ravichandran, M., McPhaden, M.J., Rao, R.R., 2011. Intraseasonal variability in barrier layer thickness in the south-central Bay of Bengal. J. Geophys. Res. 116, C03009. https://doi.org/10.1029/2010JC006657.
Gomes, H.R., Goes, J.I., Saino, T., 2000. Influence of physical processes and freshwater discharge on the seasonality of phytoplankton regime in the Bay of Bengal. Cont. Shelf Res. 20, 313–330. https://doi.org/10.1016/S0278-4343(99)00072-2.
Govil, P., Mazumder, A., Agrawal, S., Azharuddin, S., Mishra, R., Khan, H., Kumar, B., Verma, D., 2022. Abrupt changes in the southwest monsoon during Mid-Late Holocene in the western Bay of Bengal. J. Asian Earth Sci. 227, 105100. https://doi.org/10.1016/j.jseaes.2022.105100.
Greco, M., Jonkers, L., Kretschmer, K., Bijma, J., Kucera, M., 2019. Depth habitat of the planktonic foraminifera *Neogloboquadrina pachyderma* in the northern high latitudes explained by sea-ice and chlorophyll concentrations. Biogeosciences 16, 3425–3437. https://doi.org/10.5194/bg-16-3425-2019.
Guptha, M.V.S., Mohan, R., 1996. Seasonal Variability of the Vertical Fluxes of Globigerina Bulloides (d'Orbigny) in the Northern Indian Ocean, Hamburg.
Guptha, M.V.S., Curry, W.B., Ittekkot, V., Muralinath, A.S., 1997. Seasonal variation in the flux of planktic Foraminifera; sediment trap results from the Bay of Bengal, northern Indian Ocean. J. Foraminiferal Res. 27, 5–19. https://doi.org/10.2113/gsjfr.27.1.5.
Haridas, N.V., Banerji, U.S., Maya, K., Padmalal, D., 2022. Paleoclimatic and paleoceanographic records from the Bay of Bengal sediments during the last 30 ka. J. Asian Earth Sci. 229, 105169. https://doi.org/10.1016/j.jseaes.2022.105169.
Hemleben, C., Spindler, M., Anderson, O.R., 1989. Modern Planktonic Foraminifera. Springer, New York, New York, NY.
Hilbrecht, H., 1997. Morphologic gradation and ecology in *Neogloboquadrina pachyderma* and *N. dutertrei* (planktic foraminifera) from core top sediments. Mar. Micropaleontol. 31, 31–43. https://doi.org/10.1016/S0377-8398(96)00054-0.
Hood, R.R., Ummenhofer, C.C., Phillips, H.E., Sprintall, J., 2024. Introduction to the Indian Ocean®. In: Ummenhofer, C.C., Hood, R.R. (Eds.), The Indian Ocean and Its

Role in the Global Climate System. Elsevier, pp. 1–31. https://doi.org/10.1016/B978-0-12-822698-8.00015-9.
Huang, B., Jian, Z., Cheng, X., Wang, P., 2003. Foraminiferal responses to upwelling variations in the South China Sea over the last 220000 years. Mar. Micropaleontol. 47, 1–15. https://doi.org/10.1016/S0377-8398(02)00045-2.
Ittekkot, V., 1993. The abiotically driven biological pump in the ocean and short-term fluctuations in atmospheric CO2 contents. Glob. Planet. Chang. 8, 17–25. https://doi.org/10.1016/0921-8181(93)90060-2.
Iwasaki, S., Kimoto, K., Kuroyanagi, A., Kawahata, H., 2017. Horizontal and vertical distributions of planktic foraminifera in the subarctic Pacific. Mar. Micropaleontol. 130, 1–14. https://doi.org/10.1016/j.marmicro.2016.12.001.
Jonkers, L., Kučera, M., 2015. Global analysis of seasonality in the shell flux of extant planktonic Foraminifera. Biogeosciences 12, 2207–2226. https://doi.org/10.5194/bg-12-2207-2015.
Jonkers, L., Kučera, M., 2017. Quantifying the effect of seasonal and vertical habitat tracking on planktonic foraminifera proxies. Clim. Past 13, 573–586. https://doi.org/10.5194/cp-13-573-2017.
Jonkers, L., de Nooijer, L.J., Reichart, G.-J., Zahn, R., Brummer, G.-J.A., 2012. Encrustation and trace element composition of *Neogloboquadrina dutertrei* assessed from single chamber analyses – implications for paleotemperature estimates. Biogeosciences 9, 4851–4860. https://doi.org/10.5194/bg-9-4851-2012.
Jonkers, L., Laepple, T., Rillo, M.C., Shi, X., Dolman, A.M., Lohmann, G., Paul, A., Mix, A., Kucera, M., 2023. Strong temperature gradients in the ice age North Atlantic Ocean revealed by plankton biogeography. Nat. Geosci. 16, 1114–1119. https://doi.org/10.1038/s41561-023-01328-7.
Jonkers, L., Mix, A., Voelker, A., Risebrobakken, B., Smart, C.W., Ivanova, E., Arellano-Torres, E., Eynaud, F., Naoufel, H., Max, L., Rossignol, L., Simon, M.H., Martins, M.V. A., Petró, S., Caley, T., Dokken, T., Howard, W., Kucera, M., 2024. ForCenS-LGM: a dataset of planktonic foraminifera species assemblage composition for the Last Glacial Maximum. Sci. Data 11, 361. https://doi.org/10.1038/s41597-024-03166-7.
Kemle-von Mücke, S., Oberhänsli, H., 1999. The Distribution of Living Planktic Foraminifera in Relation to Southeast Atlantic Oceanography. In: Fischer, G., Wefer, G. (Eds.), Use of Proxies in Paleoceanography: Examples from the South Atlantic. Springer, Berlin, Heidelberg, pp. 91–115. https://doi.org/10.1007/978-3-642-58646-0_3.
Kennett, J.P., Huddlestun, P., 1972. Late pleistocene paleoclimatology, foraminiferal biostratigraphy and tephrochronology, western gulf of Mexico. Quat. Res. 2, 38–69. https://doi.org/10.1016/0033-5894(72)90004-X.
Kennett, J.P., Shackleton, N.J., 1975. Laurentide ice sheet meltwater recorded in gulf of mexico deep-sea cores. Science 188, 147–150. https://doi.org/10.1126/science.188.4184.147.
Khan, H., Govil, P., Panchang, R., Agrawal, S., Kumar, P., Kumar, B., Verma, D., 2023. Surface and thermocline ocean circulation intensity changes in the western Arabian Sea during ~172 kyr. Quat. Sci. Rev. 311, 108133. https://doi.org/10.1016/j.quascirev.2023.108133.
Kipp, N.G., 1976. New Transfer Function for Estimating Past Sea-Surface Conditions from Sea-Bed Distribution of Planktonic Foraminiferal Assemblages in the North Atlantic, in: Cune, R.M., Hays, J.D. (Eds.), Investigation of Late Quaternary Paleoceanography and Paleoclimatology. Geological Society of America, p. 0. https://doi.org/10.1130/MEM145-p3.
Kleijne, A., Kroon, D., Zevenboom, W., 1989. Phytoplankton and foraminiferal frequencies in northern Indian Ocean and Red Sea surface waters. Neth. J. Sea Res. 24, 531–539. https://doi.org/10.1016/0077-7579(89)90131-2.
Ko, T.W., Lee, K.E., Kim, R.A., 2025. Vertical and seasonal variations in stable oxygen isotope ratio of living planktonic foraminifera and estimation of habitat depth in the western tropical Pacific. Deep-Sea Res. I Oceanogr. Res. Pap. 216, 104440. https://doi.org/10.1016/j.dsr.2024.104440.
Kretschmer, K., Jonkers, L., Kucera, M., Schulz, M., 2018. Modeling seasonal and vertical habitats of planktonic foraminifera on a global scale. Biogeosciences 15, 4405–4429. https://doi.org/10.5194/bg-15-4405-2018.
Krishna, M.S., Prasad, M.H.K., Rao, D.B., Viswanadham, R., Sarma, V.V.S.S., Reddy, N.P. C., 2016. Export of dissolved inorganic nutrients to the northern Indian Ocean from the Indian monsoonal rivers during discharge period. Geochimica et Cosmochimica Acta 172, 430–443. https://doi.org/10.1016/j.gca.2015.10.013.
Kucera, M., 2007. Chapter six planktonic foraminifera as tracers of past oceanic environments. Develop. Marine Geol. Elsevier 213–262.
Kumar, P.K., Band, S.T., Ramesh, R., Awasthi, N., 2018. Monsoon variability and upper ocean stratification during the last ~66 ka over the Andaman Sea: Inferences from the δ 18 O records of planktonic foraminifera. Quat. Int. 479, 12–18. https://doi.org/10.1016/j.quaint.2018.03.025.
Kumari, A., Kumar, S.P., Chakraborty, A., 2018. Seasonal and interannual variability in the barrier layer of the bay of Bengal. JGR Oceans 123, 1001–1015. https://doi.org/10.1002/2017JC013213.
Kuroyanagi, A., Kawahata, H., 2004. Vertical distribution of living planktonic foraminifera in the seas around Japan. Mar. Micropaleontol. 53, 173–196. https://doi.org/10.1016/j.marmicro.2004.06.001.
Lakhani, K.Q., Lynch-Stieglitz, J., Monteagudo, M.M., 2022. Constraining calcification habitat using oxygen isotope measurements in tropical planktonic foraminiferal tests from surface sediments. Mar. Micropaleontol. 170, 102074. https://doi.org/10.1016/j.marmicro.2021.102074.
Lessa, D., Morard, R., Jonkers, L., Venancio, I.M., Reuter, R., Baumeister, A., Albuquerque, A.L., Kucera, M., 2020. Distribution of planktonic foraminifera in the subtropical South Atlantic: depth hierarchy of controlling factors. Biogeosciences 17, 4313–4342. https://doi.org/10.5194/bg-17-4313-2020.
Lévy, M., Shankar, D., André, J.-M., Shenoi, S.S.C., Durand, F., de Boyer Montégut, C., 2007. Basin-wide seasonal evolution of the Indian Ocean's phytoplankton blooms. J. Geophys. Res. Oceans 112. https://doi.org/10.1029/2007JC004090.
Lipps, J., Valentine, J., 1970. The role of foraminifera in the trophic structure of marine communities. Lethaia 3, 279–286. https://doi.org/10.1111/j.1502-3931.1970.tb01271.x.
Löscher, C.R., 2021. Reviews and syntheses: Trends in primary production in the Bay of Bengal – is it at a tipping point? Biogeosciences 18, 4953–4963. https://doi.org/10.5194/bg-18-4953-2021.
Lynch-Stieglitz, J., Polissar, P.J., Jacobel, A.W., Hovan, S.A., Pockalny, R.A., Lyle, M., Murray, R.W., Ravelo, A.C., Bova, S.C., Dunlea, A.G., Ford, H.L., Hertzberg, J.E., Wertman, C.A., Maloney, A.E., Shackford, J.K., Wejnert, K., Xie, R.C., 2015. Glacial-interglacial changes in central tropical Pacific surface seawater property gradients. Paleoceanography 30, 2014PA002746. https://doi.org/10.1002/2014PA002746.
Maeda, A., Kuroyanagi, A., Iguchi, A., Gaye, B., Rixen, T., Nishi, H., Kawahata, H., 2022. Seasonal variation of fluxes of planktic foraminiferal tests collected by a time-series sediment trap in the central Bay of Bengal during three different years. Deep-Sea Res. I Oceanogr. Res. Pap. 183, 103718.
Marino, G., Zahn, R., Ziegler, M., Purcell, C., Knorr, G., Hall, I.R., Ziveri, P., Elderfield, H., 2013. Agulhas salt-leakage oscillations during abrupt climate changes of the Late Pleistocene. Paleoceanography 28, 599–606. https://doi.org/10.1002/palo.20038.
Meilland, J., Siccha, M., Kaffenberger, M., Bijma, J., Kucera, M., 2021. Population dynamics and reproduction strategies of planktonic foraminifera in the open ocean. Biogeosciences 18, 5789–5809. https://doi.org/10.5194/bg-18-5789-2021.
Mohtadi, M., Lückge, A., Steinke, S., Groeneveld, J., Hebbeln, D., Westphal, N., 2010. Late Pleistocene surface and thermocline conditions of the eastern tropical Indian Ocean. Quat. Sci. Rev. 29, 887–896. https://doi.org/10.1016/j.quascirev.2009.12.006.
Mojtahid, M., Manceau, R., Schiebel, R., Hennekam, R., de Lange, G.J., 2014. Thirteen thousand years of southeastern Mediterranean climate variability inferred from an integrative planktic foraminiferal-based approach. Paleoceanography 30. https://doi.org/10.1002/2014PA002705. Received 29, 2.
Morard, R., Füllberg, A., Brummer, G.-J.A., Greco, M., Jonkers, L., Wizemann, A., Weiner, A.K.M., Darling, K., Siccha, M., Ledevin, R., Kitazato, H., de Garidel-Thoron, T., de Vargas, C., Kucera, M., 2019. Genetic and morphological divergence in the warm-water planktonic foraminifera genus Globigerinoides. PLoS One 14, e0225246. https://doi.org/10.1371/journal.pone.0225246.
Mortyn, P.G., Charles, C.D., 2003. Planktonic foraminiferal depth habitat and δ18O calibrations: Plankton tow results from the Atlantic sector of the Southern Ocean. Paleoceanography 18. https://doi.org/10.1029/2001PA000637.
Munir, S., Sun, J., Morton, S.L., Zhang, X., Ding, C., 2022. Horizontal Distribution and Carbon Biomass of Planktonic Foraminifera in the Eastern Indian Ocean. Water 14, 2048. https://doi.org/10.3390/w14132048.
Naidu, P.D., 1991. Glacial to interglacial contrasts in the calcium carbonate content and influence of Indus discharge in two eastern Arabian Sea cores. Palaeogeogr. Palaeoclimatol. Palaeoecol. 86, 255–263. https://doi.org/10.1016/0031-0182(91)90084-5.
Naidu, P.D., 1993. Distribution patterns of Recent planktonic foraminifera in surface sediments of the western continental margin of India. Mar. Geol. 110, 403–418. https://doi.org/10.1016/0025-3227(93)90097-F.
Narvekar, J., Prasanna Kumar, S., 2014. Mixed layer variability and chlorophyll *a* biomass in the Bay of Bengal. Biogeosciences 11, 3819–3843. https://doi.org/10.5194/bg-11-3819-2014.
Narayanan Nampoothiri, S.V., S, T.s., R, K., 2020. Dynamics and forcing mechanisms of upwelling along the south eastern Arabian sea during south west monsoon. Reg. Stud. Mar. Sci. 40, 101519. https://doi.org/10.1016/j.rsma.2020.101519.
Nürnberg, D., Bijma, J., Hemleben, C., 1996. Assessing the reliability of magnesium in foraminiferal calcite as a proxy for water mass temperatures. Geochim. Cosmochim. Acta 60, 803–814.
Oksanen, J., Simpson, G., Blanchet, F., Kindt, R., Legendre, P., Minchin, P., O'Hara, R., Solymos, P., Stevens, M., Szoecs, E., Wagner, H., Barbour, M., Bedward, M., Bolker, B., Borcard, D., Carvalho, G., Chirico, M., De Caceres, M., Durand, S., Evangelista, H., FitzJohn, R., Friendly, M., Furneaux, B., Hannigan, G., Hill, M., Lahti, L., McGlinn, D., Ouellette, M., Ribeiro Cunha, E., Smith, T., Stier, A., Ter Braak, C., Weedon, J., 2024. _vegan: Community Ecology Package_. R package version 2, 6–8. https://CRAN.R-project.org/package=vegan.
Ortiz, J.D., Mix, A.C., Collier, R.W., 1995. Environmental control of living symbiotic and asymbiotic foraminifera of the California Current. Paleoceanography 10, 987–1009. https://doi.org/10.1029/95PA02088.
Ota, Y., Kuroda, J., Yamaguchi, A., Suzuki, A., Araoka, D., Ishimura, T., Kawahata, H., 2019. Monsoon-influenced variations in plankton community structure and upper-water column stratification in the western Bay of Bengal during the past 80 ky. Palaeogeogr. Palaeoclimatol. Palaeoecol. 521, 138–150. https://doi.org/10.1016/j.palaeo.2019.02.020.
Pante, E., Simon-Bouhet, B., 2013. marmap: A Package for Importing, Plotting and Analyzing Bathymetric and Topographic Data in R, 2013. PLOS ONE 8. https://doi.org/10.1371/journal.pone.0073051.
Papa, F., Durand, F., Rossow, W.B., Rahman, A., Bala, S.K., 2010. Satellite altimeter-derived monthly discharge of the Ganga-Brahmaputra River and its seasonal to interannual variations from 1993 to 2008. J. Geophys. Res. Oceans 115. https://doi.org/10.1029/2009JC006075.
Paul, J.T., Ramaiah, N., Gauns, M., Fernandes, V., 2007. Preponderance of a few diatom species among the highly diverse microphytoplankton assemblages in the Bay of Bengal. Mar. Biol. 152, 63–75. https://doi.org/10.1007/s00227-007-0657-5.
Pédelaborde, P., 1963. The monsoon. Methuen, London, p. 196.

Peeters, F.J.C., Brummer, G.-J.A., 2002a. The seasonal and vertical distribution of living planktic foraminifera in the NW Arabian Sea. In: Clift, P.D., Kroon, D., Gaedicke, C., Craig, J. (Eds.), The Tectonic and Climatic Evolution of the Arabian Sea Region. Geological Society of London, p. 0. https://doi.org/10.1144/GSL.SP.2002.195.01.26.

Peeters, F.J.C., Brummer, G.-J.A., 2002b. The seasonal and vertical distribution of living planktic foraminifera in the NW Arabian Sea. In: Clift, P.D., Kroon, D., Gaedicke, C., Craig, J. (Eds.), The Tectonic and Climatic Evolution of the Arabian Sea Region. Geological Society of London, p. 0. https://doi.org/10.1144/GSL.SP.2002.195.01.26.

Peeters, F.J.C., Acheson, R., Brummer, G.-J.A., de Ruijter, W.P.M., Schneider, R.R., Ganssen, G.M., Ufkes, E., Kroon, D., 2004. Vigorous exchange between the Indian and Atlantic oceans at the end of the past five glacial periods. Nature 430, 661–665. https://doi.org/10.1038/nature02785.

Pracht, H., Metcalfe, B., Peeters, F.J.C., 2019a. Oxygen isotope composition of the final chamber of planktic foraminifera provides evidence of vertical migration and depth-integrated growth. Biogeosciences 16, 643–661. https://doi.org/10.5194/bg-16-643-2019.

Pracht, H., Metcalfe, B., Peeters, F.J.C., 2019b. Oxygen isotope composition of the final chamber of planktic foraminifera provides evidence of vertical migration and depth-integrated growth. Biogeosciences 16, 643–661. https://doi.org/10.5194/bg-16-643-2019.

Prasanna Kumar, S., Muraleedharan, P.M., Prasad, T.G., Gauns, M., Ramaiah, N., de Souza, S.N., Sardesai, S., Madhupratap, M., 2002a. Why is the Bay of Bengal less productive during summer monsoon compared to the Arabian Sea? Geophys. Res. Lett. 29, 2235. https://doi.org/10.1029/2002GL016013.

Prasanna Kumar, S., Muraleedharan, P.M., Prasad, T.G., Gauns, M., Ramaiah, N., de Souza, S.N., Sardesai, S., Madhupratap, M., 2002b. Why is the Bay of Bengal less productive during summer monsoon compared to the Arabian Sea? Geophys. Res. Lett. 29, 2235. https://doi.org/10.1029/2002GL016013.

Prasanna Kumar, S., Narvekar, J., Kumar, A., Shaji, C., Anand, P., Sabu, P., Rijomon, G., Josia, J., Jayaraj, K.A., Radhika, A., Nair, K.K.C., 2004. Intrusion of the Bay of Bengal water into the Arabian Sea during winter monsoon and associated chemical and biological response. Geophys. Res. Lett. 31, L15304. https://doi.org/10.1029/2004GL020247.

Prasanna Kumar, S., Narvekar, J., Nuncio, M., Kumar, A., Ramaiah, N., Sardesai, S., Gauns, M., Fernandes, V., Paul, J., 2010. Is the biological productivity in the Bay of Bengal light limited? Current Sci. 98, 1331–1339.

Prasanth, R., Vijith, V., Vinayachandran, P.N., 2023. Formation, maintenance and diurnal variability of subsurface chlorophyll maximum during the summer monsoon in the southern Bay of Bengal. Prog. Oceanogr. 212, 102974. https://doi.org/10.1016/j.pocean.2023.102974.

Raddatz, J., Nürnberg, D., Tiedemann, R., Rippert, N., 2017. Southeastern marginal West Pacific Warm Pool sea-surface and thermocline dynamics during the Pleistocene (2.5–0.5 Ma). Palaeogeogr. Palaeoclimatol. Palaeoecol. 471, 144–156. https://doi.org/10.1016/j.palaeo.2017.01.024.

van Raden, U.J., Groeneveld, J., Raitzsch, M., Kucera, M., 2011. Mg/Ca in the planktonic foraminifera *Globorotalia inflata* and *Globigerinoides bulloides* from Western Mediterranean plankton tow and core top samples. Mar. Micropaleontol. 78, 101–112. https://doi.org/10.1016/j.marmicro.2010.11.002.

Rashid, H., Flower, B.P., Poore, R.Z., Quinn, T.M., 2007. A ~25 ka Indian Ocean monsoon variability record from the Andaman Sea. Quat. Sci. Rev. 26, 2586–2597. https://doi.org/10.1016/j.quascirev.2007.07.002.

Rashid, H., England, E., Thompson, L., Polyak, L., 2011. Late glacial to Holocene Indian summer monsoon variability based upon sediment. Terr. Atmos. Ocean. Sci. 22, 215–228.

Ravelo, A.C., Andreasen, D.H., 1999. Using Planktonic Foraminifera as Monitors of the Tropical Surface Ocean. In: Abrantes, F., Mix, A.C. (Eds.), Reconstructing Ocean History. Springer US, Boston, MA, pp. 217–243. https://doi.org/10.1007/978-1-4615-4197-4_14.

Ravelo, A.C., Fairbanks, R.G., Philander, S.G.H., 1990. Reconstructing tropical Atlantic hydrography using planktontic foraminifera and an ocean model. Paleoceanography 5, 409–431. https://doi.org/10.1029/PA005i003p00409.

Rebotim, A., Voelker, A.H.L., Jonkers, L., Waniek, J.J., Meggers, H., Schiebel, R., Fraile, I., Schulz, M., Kucera, M., 2017. Factors controlling the depth habitat of planktonic foraminifera in the subtropical eastern North Atlantic. Biogeosciences 14, 827–859. https://doi.org/10.5194/bg-14-827-2017.

Regenberg, M., Nielsen, S.N., Kuhnt, W., Holbourn, A., Garbe-Schönberg, D., Andersen, N., 2010. Morphological, geochemical, and ecological differences of the extant menardiform planktonic foraminifera *Globorotalia menardii* and *Globorotalia cultrata*. Mar. Micropaleontol. 74, 96–107. https://doi.org/10.1016/j.marmicro.2010.01.002.

Rippert, N., Nürnberg, D., Raddatz, J., Maier, E., Hathorne, E., Bijma, J., Tiedemann, R., 2016. Constraining foraminiferal calcification depths in the western Pacific warm pool. Mar. Micropaleontol. 128, 14–27. https://doi.org/10.1016/j.marmicro.2016.08.004.

Rodríguez-Sanz, L., Bernasconi, S.M., Marino, G., Heslop, D., Müller, I.A., Fernandez, A., Grant, K.M., Rohling, E.J., 2017. Penultimate deglacial warming across the Mediterranean Sea revealed by clumped isotopes in foraminifera. Sci. Rep. 7, 16572. https://doi.org/10.1038/s41598-017-16528-6.

Rohling, E.J., Sprovieri, M., Cane, T., Casford, J.S.L., Cooke, S., Bouloubassi, I., Emeis, K. C., Schiebel, R., Rogerson, M., Hayes, A., Jorissen, F.J., Kroon, D., 2004. Reconstructing past planktic foraminiferal habitats using stable isotope data: a case history for Mediterranean sapropel S5. Mar. Micropaleontol. 50, 89–123. https://doi.org/10.1016/S0377-8398(03)00068-9.

Salmon, K.H., Anand, P., Sexton, P.F., Conte, M., 2015. Upper ocean mixing controls the seasonality of planktonic foraminifer fluxes and associated strength of the carbonate pump in the oligotrophic North Atlantic. Biogeosciences 12, 223–235. https://doi.org/10.5194/bg-12-223-2015.

Sánchez, A., Carriquiry, J., 2024. Thermocline-level connectivity between the tropical equatorial Pacific and tropical northeast Pacific during deglaciation. Quat. Int. 705, 86–93. https://doi.org/10.1016/j.quaint.2024.03.010.

Saraswat, R., Khare, N., 2010. Deciphering the modern calcification depth of Globigerina bulloides in the southwestern Indian Ocean from its oxygen isotopic composition. J. Foraminifer. Res. 40, 220–230. https://doi.org/10.2113/gsjfr.40.3.220.

Saraswat, R., Nigam, R., Li, T., Griffith, E.M., 2017. Marine paleoclimatic proxies: A shift from qualitative to quantitative estimation of seawater parameters. Palaeogeography, Palaeoclimatology, Palaeoecology, Development, evaluation and application of marine paleoclimatic/paleoceanographic proxies: An update 483, 1–5.

Sarma, V.V.S.S., Rao, G.D., Viswanadham, R., Sherin, C.K., Salisbury, J., Omand, M., Mahedevan, A., Murty, V.S.N., Shroyer, E., Baumgartner, M., Stafford, K., 2016. Effects of freshwater stratification on nutrients, dissolved oxygen, and phytoplankton in the bay of Bengal. Oceanography 29, 222–231. https://doi.org/10.5670/oceanog.2016.54.

Schiebel, R., 2002. Planktic foraminiferal sedimentation and the marine calcite budget. Glob. Biogeochem. Cycles 16. https://doi.org/10.1029/2001GB001459.

Schiebel, R., Hemleben, C., 2017. Planktic Foraminifers in the Modern Ocean. Springer Berlin Heidelberg, Berlin, Heidelberg. https://doi.org/10.1007/978-3-662-50297-6.

Schiebel, R., Waniek, J., Bork, M., Hemleben, C., 2001. Planktic foraminiferal production stimulated by chlorophyll redistribution and entrainment of nutrients. Deep-Sea Res. I Oceanogr. Res. Pap. 48, 721–740. https://doi.org/10.1016/S0967-0637(00)00065-0.

Schlitzer, R., 2023. Ocean Data View.

Schmuker, B., 2000. Recent Planktic Foraminifera in the Caribbean Sea. ETH Zürich.

Schmuker, B., Schiebel, R., 2002. Planktic foraminifers and hydrography of the eastern and northern Caribbean Sea. Mar. Micropaleontol. 46, 387–403. https://doi.org/10.1016/S0377-8398(02)00082-8.

Schott, F.A., McCreary Jr., J.P., 2001. The monsoon circulation of the Indian Ocean. Prog. Oceanogr. 51, 1–123. https://doi.org/10.1016/S0079-6611(01)00083-0.

Schott, F.A., Xie, S.-P., McCreary, J.P., 2009. Indian Ocean circulation and climate variability. Rev. Geophys. 47. https://doi.org/10.1029/2007RG000245.

Seears, H.A., Darling, K.F., Wade, C.M., 2012. Ecological partitioning and diversity in tropical planktonic foraminifera. BMC Evol. Biol. 12, 54. https://doi.org/10.1186/1471-2148-12-54.

Shankar, D., Vinayachandran, P.N., Unnikrishnan, A.S., 2002. The monsoon currents in the north Indian Ocean. Prog. Oceanogr. 52, 63–120. https://doi.org/10.1016/S0079-6611(02)00024-1.

Shenoi, S.S.C., Shankar, D., Shetye, S.R., 2002. Differences in heat budgets of the near-surface Arabian Sea and Bay of Bengal: Implications for the summer monsoon. J. Geophys. Res. 107, 5–11. https://doi.org/10.1029/2000JC000679.

Shetye, S.R., Shenoi, S.S.C., Gouveia, A.D., Michael, G.S., Sundar, D., Nampoothiri, G., 1991. Wind-driven coastal upwelling along the western boundary of the Bay of Bengal during the southwest monsoon. Cont. Shelf Res. 11, 1397–1408. https://doi.org/10.1016/0278-4343(91)90042-5.

Shetye, S.R., Gouveia, A.D., Shenoi, S.S.C., Sundar, D., Michael, G.S., Nampoothiri, G., 1993. The western boundary current of the seasonal subtropical gyre in the Bay of Bengal. J. Geophys. Res. 98, 945–954. https://doi.org/10.1029/92JC02070.

Siccha, M., Kucera, M., 2017. ForCenS, a curated database of planktonic foraminifera census counts in marine surface sediment samples. Sci. Data 4, 170109. https://doi.org/10.1038/sdata.2017.109.

Singh, A., Ramesh, R., 2011. Contribution of riverine dissolved inorganic nitrogen flux to new production in the coastal northern Indian ocean: An assessment. Int. J. Oceanogr. 2011, 983561. https://doi.org/10.1155/2011/983561.

Singh, S.P., Singh, S.K., Goswami, V., Bhushan, R., Rai, V.K., 2012. Spatial distribution of dissolved neodymium and εNd in the Bay of Bengal: Role of particulate matter and mixing of water masses. Geochim. Cosmochim. Acta 94, 38–56. https://doi.org/10.1016/j.gca.2012.07.017.

Siswanto, E., Sarker, M.L.R., Peter, B.N., Takemura, T., Horii, T., Matsumoto, K., Taketani, F., Honda, M.C., 2023. Variations of phytoplankton chlorophyll in the Bay of Bengal: Impact of climate changes and nutrients from different sources. Front. Mar. Sci. 10. https://doi.org/10.3389/fmars.2023.1052286.

Spero, H.J., Lea, D.W., 1993. Intraspecific stable isotope variability in the planktic foraminiferaGlobigerinoides sacculifer: Results from laboratory experiments. Mar. Micropaleontol. 22, 221–234. https://doi.org/10.1016/0377-8398(93)90045-Y.

Spero, H.J., Lea, D.W., 2002. The cause of carbon isotope minimum events on glacial terminations. Science 296, 522–525. https://doi.org/10.1126/science.1069401.

Stainbank, S., Kroon, D., Rüggeberg, A., Raddatz, J., de Leau, E.S., Zhang, M., Spezzaferri, S., 2019. Controls on planktonic foraminifera apparent calcification depths for the northern equatorial Indian Ocean. PLoS One 14, e0222299. https://doi.org/10.1371/journal.pone.0222299.

Stoll, H.M., Arevalos, A., Burke, A., Ziveri, P., Mortyn, G., Shimizu, N., Unger, D., 2007. Seasonal cycles in biogenic production and export in Northern Bay of Bengal sediment traps. Deep Sea Res. Part II: Topical Stud. Oceanogr. 54, 558–580. https://doi.org/10.1016/j.dsr2.2007.01.002.

Sykes, F.E., Meilland, J., Westgård, A., Chalk, T.B., Chierici, M., Foster, G.L., Ezat, M.M., 2024. Large-scale culturing of the subpolar foraminifera Globigerina bulloides reveals tolerance to a large range of environmental parameters associated to different life-strategies and an extended lifespan. J. Plankton Res. 46, 403–420. https://doi.org/10.1093/plankt/fbae029.

Takagi, H., Moriya, K., Ishimura, T., Suzuki, A., Kawahata, H., Hirano, H., 2016. Individual migration pathways of modern planktic foraminifers: chamber-by-

chamber assessment of stable isotopes. JPAL 20, 268–284. https://doi.org/10.2517/2015PR036.
Takagi, H., Kimoto, K., Fujiki, T., Saito, H., Schmidt, C., Kucera, M., Moriya, K., 2019. Characterizing photosymbiosis in modern planktonic foraminifera. Biogeosciences 16, 3377–3396. https://doi.org/10.5194/bg-16-3377-2019.
Tapia, R., Ho, S.L., Wang, H.-Y., Groeneveld, J., Mohtadi, M., 2022. Contrasting vertical distributions of recent planktic foraminifera off Indonesia during the southeast monsoon: implications for paleoceanographic reconstructions. Biogeosciences 19, 3185–3208. https://doi.org/10.5194/bg-19-3185-2022.
Thadathil, P., Muraleedharan, P.M., Rao, R.R., Somayajulu, Y.K., Reddy, G.V., Revichandran, C., 2007. Observed seasonal variability of barrier layer in the Bay of Bengal. J. Geophys. Res. 112, C02009. https://doi.org/10.1029/2006JC003651.
Thunell, R.C., 1976. Calcium carbonate dissolution history in late quaternary deep-sea sediments, Western Gulf of Mexico. Quat. Res. 6, 281–297. https://doi.org/10.1016/0033-5894(76)90055-7.
Thunell, R.C., 1978. Distribution of recent planktonic foraminifera in surface sediments of the Mediterranean Sea. Mar. Micropaleontol. 3, 147–173. https://doi.org/10.1016/0377-8398(78)90003-8.
Thunell, R.C., Reynolds, L.A., 1984. Sedimentation of planktonic foraminifera: seasonal changes in species flux in the panama basin. Micropaleontology 30, 243–262. https://doi.org/10.2307/1485688.
Thunell, R.C., Williams, D.F., Kennett, J.P., 1977. Late Quaternary paleoclimatology, stratigraphy and sapropel history in eastern Mediterranean deep-sea sediments. Mar. Micropaleontol. 2, 371–388. https://doi.org/10.1016/0377-8398(77)90018-4.
Thushara, V., Vinayachandran, P.N.M., Matthews, A.J., Webber, B.G.M., Queste, B.Y., 2019. Vertical distribution of chlorophyll in dynamically distinct regions of the southern Bay of Bengal. Biogeosciences 16, 1447–1468. https://doi.org/10.5194/bg-16-1447-2019.
Ufkes, E., Fred Jansen, J.H., Brummer, G.-J.A., 1998. Living planktonic foraminifera in the eastern South Atlantic during spring: Indicators of water masses, upwelling and the Congo (Zaire) River plume. Mar. Micropaleontol. 33, 27–53. https://doi.org/10.1016/S0377-8398(97)00032-7.
Umling, N.E., Thunell, R.C., 2017. Synchronous deglacial thermocline and deep-water ventilation in the eastern equatorial Pacific. Nat. Commun. 8, 14203. https://doi.org/10.1038/ncomms14203.
Verma, K., Singh, H., Singh, A.D., Singh, P., Satpathy, R.K., Naidu, P.D., 2021. Benthic foraminiferal response to the millennial-scale variations in monsoon-driven productivity and deep-water oxygenation in the western bay of bengal during the Last 45 ka. Front. Mar. Sci. 8. https://doi.org/10.3389/fmars.2021.733365.
Verma, K., Singh, A.D., Singh, P., Singh, H., Satpathy, R.K., Uddandam, P.R., Naidu, P.D., 2022. Monsoon-related changes in surface hydrography and productivity in the Bay of Bengal over the last 45 kyr BP. Palaeogeogr. Palaeoclimatol. Palaeoecol. 589, 110844. https://doi.org/10.1016/j.palaeo.2022.110844.
Vinayachandran, P.N., 2002. Observations of barrier layer formation in the Bay of Bengal during summer monsoon. J. Geophys. Res. 107. https://doi.org/10.1029/2001JC000831.
Vinayachandran, P.N., 2009. Impact of physical processes on chlorophyll distribution in the Bay of Bengal. In: Wiggert, J.D., Hood, R.R., Naqvi, S.W.A., Brink, K.H., Smith, S. L. (Eds.), Geophysical Monograph Series. American Geophysical Union, Washington, D. C., pp. 71–86. https://doi.org/10.1029/2008GM000705
Vinayachandran, P.N., Masumoto, Y., Mikawa, T., Yamagata, T., 1999. Intrusion of the Southwest Monsoon Current into the Bay of Bengal. J. Geophys. Res. 104, 11077–11085. https://doi.org/10.1029/1999JC900035.
Vinayachandran, P.N.M., Masumoto, Y., Roberts, M.J., Huggett, J.A., Halo, I., Chatterjee, A., Amol, P., Gupta, G.V.M., Singh, A., Mukherjee, A., Prakash, S., Beckley, L.E., Raes, E.J., Hood, R., 2021. Reviews and syntheses: Physical and biogeochemical processes associated with upwelling in the Indian Ocean. Biogeosciences 18, 5967–6029. https://doi.org/10.5194/bg-18-5967-2021.
Vinayachandran, P.N., Mathew, S., 2003. Phytoplankton bloom in the Bay of Bengal during the northeast monsoon and its intensification by cyclones. Geophys. Res. Lett. 30. https://doi.org/10.1029/2002GL016717.
Vinayachandran, P.N., McCreary Jr., J.P., Hood, R.R., Kohler, K.E., 2005. A numerical investigation of the phytoplankton bloom in the Bay of Bengal during Northeast Monsoon. J. Geophys. Res. Oceans 110. https://doi.org/10.1029/2005JC002966.
Wang, L., 2000. Isotopic signals in two morphotypes of Globigerinoides ruber (white) from the South China Sea: implications for monsoon climate change during the last glacial cycle. Palaeogeogr. Palaeoclimatol. Palaeoecol. 161, 381–394.
Watkins, J.M., Mix, A.C., Wilson, J., 1996. Living planktic foraminifera: tracers of circulation and productivity regimes in the central equatorial Pacific. Deep-Sea Res. II Top. Stud. Oceanogr. 43, 1257–1282. https://doi.org/10.1016/0967-0645(96)00008-2.
Wickham, H., Chang, W., Henry, L., Pedersen, T.L., Takahashi, K., Wilke, C., Woo, K., Yutani, H., Dunnington, D., van den Brand, T., 2025. ggplot2: Elegant Graphics for Data Analysis.
Wilke, I., Meggers, H., Bickert, T., 2009. Stable Oxygen Isotope Composition of Planktonic Foraminifera in the Canary Islands Region.
Yang, H., Wang, F., 2009. Revisiting the thermocline depth in the equatorial pacific. J. Clim. 22, 3856–3863. https://doi.org/10.1175/2009JCLI2836.1.
Yu, Z., Colin, C., Meynadier, L., Douville, E., Dapoigny, A., Reverdin, G., Wu, Q., Wan, S., Song, L., Xu, Z., Bassinot, F., 2017. Seasonal variations in dissolved neodymium isotope composition in the Bay of Bengal. Earth Planet. Sci. Lett. 479, 310–321. https://doi.org/10.1016/j.epsl.2017.09.022.
Zar, J., 2014. Biostatistical Analysis, Fifth edition. Pearson New International Edition. 978-1-292-02404-2.
Zhang, J., 1985. Living planktonic foraminifera from the eastern Arabian Sea. Deep Sea Research Part A. Oceanographic Res. Papers 32, 789–798. https://doi.org/10.1016/0198-0149(85)90115-3.